Linking regional shifts in microbial genome adaptation with surface ocean biogeochemistry

Authors: Catherine A. Garcia¹, George I. Hagstrom², Alyse A. Larkin¹, Lucas J. Ustick³, Simon A. Levin², Michael W. Lomas⁴, Adam C. Martiny^{1,3*}

- Department of Earth System Science, University of California, Irvine, California 92697, USA
 Department of Ecology and Evolutionary Biology, Princeton University, Princeton, New Jersey 08544, USA
- 3. Department of Ecology and Evolutionary Biology, University of California, Irvine, California 92697, USA
 - 4. Bigelow Laboratory for Ocean Sciences, East Boothbay, Maine 04544, USA

Keywords: Metagenomics, Redfield Ratio, elemental stoichiometry

Main Text

Summary

Linking 'omics measurements with biogeochemical cycles is a widespread challenge in microbial community ecology. Here, we propose applying genomic adaptation as 'biosensors' for microbial investments to overcome nutrient stress. We then integrate this genomic information with a trait-based model to predict regional shifts in the elemental composition of marine plankton communities. We evaluated this approach using metagenomic and particulate organic matter samples from the Atlantic, Indian, and Pacific Ocean. We find that our genome-based trait-model significantly improves our prediction of particulate C:P (carbon: phosphorus) across ocean regions. Furthermore, we detect previously unrecognized ocean areas of iron, nitrogen, and phosphorus stress. In many ecosystems, it can be very challenging to quantify microbial stress. Thus, a carefully calibrated genomic approach could become a widespread tool for understand microbial responses to environmental changes and the biogeochemical outcomes.

Introduction

Linking genomics and other 'omics measurements with biogeochemical cycles is a widespread challenge in microbial community ecology. Currently, most 'omics observations are used to quantify shifts in diversity and functional potential. In contrast, we rarely use microbial 'omics data to understand and constrain large-scale energy or nutrient fluxes. This lack of convergence between microbial 'omics information and ecosystem or global models may limit our ability to predict future changes to global biogeochemical cycles.

It is well-established that the cellular and community regulation of elemental requirements and composition (i.e., carbon: nitrogen: phosphorus, C:N:P) are important for linking the global carbon and nutrient cycles [1]. There is an intense debate about the interaction between microbial diversity and environmental changes in regulating C:N:P for both terrestrial and aquatic environments [1,2]. The chemical composition of a cell is affected by many environmental factors, but nutrient availability is emerging as central [3]. Nutrient availability impacts the elemental composition of a community in multiple ways. Physiologically, the overall nutrient level impacts the growth rate [4]. In addition, cells are sensitive to the supply ratio of N vs. P (and other nutrients) relative to the biomass ratio [5]. Microbial lineages can also have unique resource requirements and thus experience a shared environment differently at a physiological level. For example, the marine cyanobacterium *Prochlorococcus* appears to have a lower P requirement compared to larger phytoplankton [6] and co-existing diatoms can have unique N:P [7]. Thus, the interaction between microbial diversity and nutrient stress plays a complex role in regulating ecosystem C:N:P.

It is a challenge to define and quantify the nutritional environment experienced by microorganisms. First, the concentrations of inorganic phosphorus and nitrogen are commonly below detection limits in many marine environments [8]. Second, most microorganisms can utilize multiple alternative forms of nutrients [9–12]. Ammonium is energetically the most favored form of nitrogen. When ammonium is in low supply, microorganisms can shift in some order to urea, nitrate, or organically bound nitrogen [13]. There are several unknowns associated with the use of alternative resources. We rarely quantify the concentration and chemical form of alternative nutrients or the chemical nature of organically bound N or P. Either assumptions are made about what substrate microorganisms are using, or there are difficulties obtaining isotopically labelled compounds for more complex alternative nutrient sources making it a challenge to evaluate their role. Furthermore, the resource costs associated with the use of many alternative nutrients are broadly unknown, leading to ill-defined trade-offs for nutrient assimilation. For example, cells need to invest N when upregulating acquisition proteins leading to trade-offs between nutrient investments and uptake [14]. Finally, there is variation among individual lineages

in the extent they can rely on alternative nutrient forms [15]. Thus, it is currently impossible to predict microbial nutrient use and associated biogeochemical roles even with a perfect chemical characterization of an environment.

Marine microorganisms show clear genomic evidence for adaptation to specific nutritional environments through gene gain and loss [16–18]. Such genomic changes reflect a shift from simple to more complex nutrient forms under limiting conditions. This pattern has been detected in many microorganisms but is clearly illustrated in marine cyanobacteria. In regions with a replete inorganic phosphate supply, *Prochlorococcus* genomes mainly contain transporters directly associated with inorganic phosphate [19]. However, *Prochlorococcus* adapts to low phosphate supply via the gain of genes associated with regulation and the use of alternative forms. In regions with severe P stress, *Prochlorococcus* genomes contain genes for alkaline phosphate to cleave off phosphate from organic molecules [20,21]. Here, alkaline phosphatase and a few other proteins can be highly induced to utilize organic P as an alternative P source [19,22]. *Prochlorococcus* adapts to N stress in a parallel fashion, whereby cells from high N areas only contain genes for ammonium uptake [23]. In regions with stronger N stress, *Prochlorococcus* genomes sequentially include genes for urea, nitrite and ultimately nitrate assimilation. Thus, the genome content of *Prochlorococcus* (and other marine microorganisms) closely corresponds to the underlying environmental conditions and thereby describes the cellular strategies for nutrient acquisition [24].

We propose using genomic shifts among microbial communities as a 'biosensor' for *in situ* nutritional environments in order to improve predictions of C:N:P variability across ocean regions. Specifically, we combine the distribution of genes with a trait model to simulate cellular investment strategies and predict C:N:P. We assume that genome streamlining in Cyanobacteria will lead to clear nutrient investment trends. However, increasing cell genomes sizes in the larger Cyanobacteria, *Synechococcus*, reveals a more generalist lifestyle. We show that in comparison to both traditional abiotic and common trait models, the incorporation of nutrient trait variation quantified using metagenomics greatly improves our ability to predict shifts in C:N:P. This work illustrates how we can use 'omics observations to improve our understanding of global biogeochemical cycles in ways that would be challenging to achieve with abiotic characterizations alone.

Methods

Sample collection

Seawater samples were collected from the western Atlantic Ocean (AE1319 – Aug/Sep 2013, BV46 – Oct 2011), central Pacific Ocean (NH1418 – Sept 2014), and the eastern Indian Ocean (IO9N – Mar/Apr 2016) (Supplementary Figure 1; Supplementary Table 1). On each cruise samples for DNA, flow cytometry, particulate organic matter, uptake rate kinetics, and nutrients were collected as described previously [3,25–28]. Fifty-four stations were selected for metagenomics analysis where these corresponding measurements were taken. Select data is already available on BCO-DMO (uptake rate kinetics, nutrient concentrations, cell abundances, and particulate elemental concentrations) for the Atlantic AE1319 and BV46 (https://www.bco-dmo.org/project/2178) and Indian Ocean I09N cruises (https://www.bco-dmo.org/project/2178) and Indian Ocean I09N cruises (https://www.bco-dmo.org/project/628972). Results have previously been reported describing the cyanobacterial diversity [28,29], cell quotas and abundances [26,27], uptake rate kinetics [25,26], and particulate organic matter ratios [3] along several transects.

Particulate organic matter

All particulate organic matter samples for carbon, nitrogen and phosphorus were collected on precombusted (4 hours at 500°C) GF/F filters with a nominal pore size of 0.7 μm. A nylon mesh prefilter with a pore size of 30 μm was used to remove rarer biomass to remove larger plankton and particles. POP filters were rinsed with 0.17M Na₂SO₄ at time of collection to remove residual dissolved organic phosphorus. All filters were stored frozen until analysis in lab. POC/PON samples were measured using a Flash 1112 EA elemental analyzer (Thermo Scientific, Waltham, MA, USA) for the I09 transect against an Atropine (C₁₇H₁₂NO₅) standard curve (range 0.2-1.5 mg). For the NH1418, AE1319, and BV46 transects POC/PON samples were measured on either Control Equipment 240-XA or 440-XA elemental analyzer using acetanilide as a standard [30]. POP samples were analyzed using an ash/hydrolysis colorimetric method described previously [31]. Briefly, 2 mL of 0.017M MgSO₄ was added to the filter and KH.PO₄ standards in acid-washed scintillation vials and dried overnight at 90°C. The filters were exposed to high

temperatures 500°C for 2 hours and acidified in 0.2M HCL at 90°C. After a mixed reagent was added, the samples were analyzed on a spectrophotometer at 885nm.

Uptake rate kinetics

On the Atlantic (AE1319, BV46) and Pacific (NH1418) Ocean transects, phosphate uptake rate kinetics were taken for whole community and taxa-specific groups (e.g. *Synechococcus* & *Prochlorococcus*) using methods previously described [25]. Incubations were performed using 10 mL seawater aliquots within 3°C of ambient temperature during time of collection (~23°C). Kinetics experiments for phosphate were performed with increasing DIP additions up to 100nM, and ended at a final concentration of 100uM.

On the Indian Ocean GO-SHIP transect (I09N), whole community bottle incubations were performed for uptake of "N-labeled ammonia, urea, and nitrate [26]. The incubations were performed in 2L polycarbonate bottles over a 6-hr period at ambient seawater temperature. N incubations were mixed to a final concentration of $0.03\mu M$, which is below the detection limit and reflective of the N-limiting conditions throughout the I09N transect.

Cell abundances using flow cytometry

Samples for flow cytometry and cell sorting were collected previously and are presented elsewhere [26–28]. Briefly, the samples were sorted using a FACSJazz or Influx flow cytometer (BD, Franklin Lakes, NJ, USA). Samples were preserved using a 0.5% paraformaldehyde solution (final concentration), kept in the dark for 1 hour to fix at 5°C, and then stored frozen at -80°C until analysis. Populations of *Synechococcus* were determined with a gate in orange (585nm), *Prochlorococcus* based on forward scatter and red fluorescence.

Nutrients

For the NH1418, AE1319, and BV46 cruises, phosphate was measured using the MAGIC-SRP high sensitivity method [32]. Nitrate was measured as using a cadmium reduction assay as previously described [28].

Nutrients data for the I09N cruise were provided by Jim Swift/SIO and Susan Becker/SIO and are available at https://cchdo.ucsd.edu.

Metagenomics – library and sequencing

For DNA, 4-10 L seawater samples were collected with a 0.22 μm Sterivex filter and preserved with Lysis Buffer (50 mM Tris -HCl pH 7.6, 20 mM EDTA pH 8.0, 400 mM NaCl, 0.75 M sucrose) and frozen at -80°C until further processing. Whereas a GF/D (2.7 μ m nominal pore size) glass fiber prefilter was used for all Pacific and Atlantic sites [28], no prefilter was used for DNA collections for Indian Ocean sites. As a minor percentage of the total community composed of eukaryotes [26], we assumed this was an acceptable comparison. However, it is possible that we are missing particle associations greater than 2.7 μm in the Atlantic and Pacific Ocean. DNA was extracted as described previously [28,33,34] and diluted (Atlantic/Pacific: $0.5 \text{ng}/\mu l$, Indian: $1 \text{ng}/\mu l$) for sequencing. Metagenomic libraries were prepared using Nextera Library Prep Kit (Illumina, San Diego, CA) with a modified PCR mixture. 1 ul was 0.5-1ng of DNA was tagmented using the Nextera DNA Prep Kit tagmentation enzyme and incubated for 10 minutes at 55°C. The Nextera XT barcodes were annealed to metagenome fragments using the following PCR protocol. For PCR, we used 20µl of a master mix containing 0.5 µL Phusion High Fidelity buffer (New England Biolabs, Ipswich, MA), 0.5 µL dNTPs (New England Biolabs, Ipswich, MA), 0.25 µL Phusion High Fidelity polymerase (New England Biolabs, Ipswich, MA), and 14.25 μL of PCR water. Equimolar samples were pooled and the quality was checked and quantified using a Bioanalyzer (Agilent, Santa Clara, CA). The pooled library was sequenced on an HiSeq - 4000 (Illumina, San Diego, CA) producing paired end reads (2 x 150 bp). Low quality reads and adapters were removed using trimmomatic 0.35 [35] with a sliding window of 4:15 and minimum length set to 36. PhiX was filtered out using BBduk2 tool BBMap (BBMap - Bushnell B. - sourceforge.net/projects/bbmap/, k = 31, hdist = 1). Sequences were aligned and mapped to a curated reference database (Supplementary Table 4) using Bowtie2 [36] with the following settings; --local -D 15 -R 2 -L 15 -N 1 --gbar 1 --mp 3. High quality contigs were assembled and processed with Anvi'o [37]. Pangenome gene clusters were identified using the DIAMOND algorithm [38] and summarized in Anvi'o. Metagenomes are available through BioProject (SRA PRJNA598881) at the following link: https://www.ncbi.nlm.nih.gov/sra/PRJNA598881.

Prochlorococcus and Synechococcus genes associated with assimilation for iron, nitrogen, and phosphorus were identified based on prior studies (Supplementary Information 1) [17,21,23,24,39,40]. Several genes of unknown function are listed as <code>uknX</code>, but are included due to their association with low P availability in <code>Prochlocococcus</code> [41], and close proximity to known regulatory P assimilation genes in the MED4 genome. Based on these past studies, we filtered out genes if present in all <code>Synechococcus</code> and <code>Prochlorococcus</code> to detect variation in lineage coverage. We found the relative gene frequency by scaling to the median coverage of single copy core genes (SCCG) [41] across 54 stations. We identified the relative gene frequency for each nutrient listed in Supplementary Information 1, per station, and per taxa (<code>Synechococcus</code> and <code>Prochlorococcus</code>) as follows:

$$relative \ gene \ frequency_{gene \ in \ taxa} = \sum_{\substack{genomes \\ in \ taxa}} \left[\left(\frac{gene \ coverage_{gene}}{median \ coverage \ of \ SCCG_{taxa}} \right) \left(\frac{total \ reads_{genome}}{total \ reads_{taxa}} \right) \right]$$

Next, we conducted three separate Principle Component Analysis (PCA) for N, P, and Fe assimilation genes, respectively (Supplementary Figure 4). Each relative gene frequency was scaled between 0 and 1 across the 54 stations as inputs to the PCA ($n \times m$ matrix of n stations and m normalized gene frequencies). A total of four gene indices were produced for each station, where N/P gene = first component of PCA;

 $N_{
m gene\ Prochlorococcus}$ $P_{
m gene\ Synechococcus}$ $N_{
m gene\ Prochlorococcus}$ $P_{
m gene\ Synechococcus}$

These N and P gene indices for *Prochlorococcus* and *Synechococcus* were subsequently incorporated into an trait model to predict C:P.

ATOM-gene Model

We developed the ATOM-gene model to predict phytoplankton C:P ratios from temperature, irradiance, and metagenomic data on phosphorus and nitrogen nutrient-uptake gene abundance. The ATOM-gene model shares its basic structure with the trait-based phytoplankton model developed by Moreno et. al. [42]. It predicts the C:P of particulate organic matter in the surface ocean using a multi-step process. ATOM-gene first characterizes phytoplankton according to several key functional traits, namely their radius (r) and their allocation of biomass to biosynthetic proteins and ribosomes (E), to photosynthetic proteins (L), to structural components (S), and to nutrient uptake proteins (A). ATOM-gene also represents a luxury nutrient storage pool. Each trait-combination corresponds both to a functional response to environmental conditions, and to a cell quotas of C, N, and P, which we derived from biophysics, physiology, and statistical modeling. The functional response determines the growth rate of cells with each trait-combination (r, E, L, A) in each possible environment, which consist of temperature (T), irradiance (L), and metagenomic uptake gene abundance indices Pgene and Ngene. Traditionally, in trait-based phytoplankton models, the functional response to environmental conditions requires nutrient concentrations to calculate growth rates. However, nitrate + nitrite and phosphate nutrient concentrations are frequently below standard assay detection limits. Furthermore, nutrient concentrations were not great predictors across regions. Therefore, we needed genes to detect unseen nutrient stress variability. Here, we treat nutrient concentrations as latent variables, which are not directly observed, and model their concentration using the metagenomic data.

Given the irradiance, temperature, and nutrient-uptake gene abundances in a given sampling location, ATOM-gene uses the functional responses to determine the trait-combination with the fastest growth rate, and predicts that these traits and the resulting C:P characterize the plankton community and particulate organic matter at that sampling site.

ATOM-gene is part of a family of trait-based models that we have developed to predict C:P ratios in phytoplankton, and which extend the model in Moreno et. al. [42] in important ways. First, ATOM-gene does not just model phosphorus availability like [42], but also models nitrogen availability. ATOM-gene includes an additional resource investment pool, representing variable allocations of biomass to surface membrane and periplasmic proteins for nutrient uptake of phosphorus. Lastly, we parameterized the trait-based model in [42] using point estimates of physiological parameters taken from the literature, only

using statistical methods to predict luxury P-storage. Here we integrated the entire ATOM-gene model into a Bayesian statistical framework, allowing us to incorporate uncertainty in our understanding of key physiological processes (such as the temperature dependence or different biochemical processes).

Below we describe the model and its parameters. Summaries of the model parameters, and the prior distributions for statistical parameters, can be found in Supplementary Tables 5, 6 and 7. Phytoplankton traits determine C:P according to:

$$(P:C) = \frac{EP_E + \gamma P_{\gamma} + P_{\text{stor}}}{EC_P + LC_P + \gamma C_{\gamma} + \frac{\alpha(C_M + AC_P)}{2r}}.$$

Here P:C is the phosphorus to carbon ratio. P_E and P_γ are the specific fraction of phosphorus in the biosynthetic protein and structure pool, respectively, with units of gP/g. Their phosphorus content arises from ribosomes in the case of the biosynthetic apparatus, which we model as having a ribosome fraction of α_E , and DNA/RNA in the case of the structural pool, which we model as occupying a total fraction γ_{DNA} of cellular biomass. P_{stor} is the level of luxury P storage, in units of gP/g. The symbol C_P is the specific fraction of carbon in proteins, with units of gC/g, C_{DNA} is the specific fraction of carbon in DNA, and C_{lip} is the specific fraction of carbon in carbon in lipids, and γ_{lip} is the fraction of cellular biomass in lipids. The fraction of cellular biomass in the inner and outer membranes and periplasmic space is $\frac{\alpha}{r'}$, which we assume is half membrane and half periplasmic space. A is the fraction of the periplasmic space occupied by proteins. C_M is the carbon fraction of the inner and outer membranes, which we assume are composed partially of proteins and partially of phospholipids. mol_P and mol_C are the molar masses of phosphorus and carbon.

The traits must satisfy several constraints. The sum of allocations to cytoplasmic components should equal the cytoplasmic fraction of the cell:

$$E + L + \gamma_{\text{\tiny DNA}} + \gamma_{\text{\tiny N}} = 1 - \frac{\alpha}{r}$$

Furthermore, the fraction of the periplasmic volume allocated to proteins satisfies $2rA_{min} < A < 1$.

To predict the stoichiometry in a given environment, ATOM-gene selects the trait combination with the fastest growth rates. Environmental conditions and traits translate into rates of biosynthesis μ_E , photosynthesis μ_L , nitrogen uptake μ_N , and phosphorus uptake μ_P , with overall growth rate determined by the slowest of these processes:

 $\mu = \min(\mu_E, \mu_L, \mu_N, \mu_P).$

The biosynthesis rate depends linearly on the investment E:

$$\mu_E = k_S(T) E,$$

where the biosynthetic efficiency decreases with temperature with a $Q_{10k} = 2$. The photosynthesis functional response comes from Geider et. al. (see the formulation Moreno et. al. 2018):

$$\mu_L = \frac{f(I,T)L}{1 + \phi_S},$$

where we allow the photosynthesis rate to have a non-trivial temperature dependence. Here T is the temperature in degrees centigrade, I is the irradiance measured in μ molPhotons/ m^2/s , and φ_S is the carbon cost of synthesis in gC/gC. The functional response f(I,T) to light is described in Moreno et. al. 2018, and depends on temperature according to a $Q_{10,photo}$. We assume diffusion-limited growth to derive the nitrogen and phosphorus dependent growth rates:

$$\begin{split} \mu_{\mathrm{N}} &= \frac{4\pi D_{\mathrm{N}}[\mathrm{N}_{\mathrm{model}}]r}{Q_{\mathrm{N}}}, \mu_{\mathrm{P}} = \frac{4\pi D_{\mathrm{P}}[\mathrm{P}_{\mathrm{model}}]rA}{Q_{\mathrm{P}}}. \\ Q_{N} &= \frac{4\pi r^{3}\mathrm{mol}_{\mathrm{N}}}{\rho p_{dry}\left(\left(E + L + \alpha A/(2r)\right)\mathrm{N}_{\mathrm{prot}} + \gamma_{\mathrm{DNA}} \ \mathrm{N}_{\mathrm{DNA}} \ + \alpha/(2r)\mathrm{N}_{\mathrm{M}}\right)} \end{split}$$

$$Q_{\rm P} = \frac{4\pi r^3 \mathrm{mol_P}}{\rho p_{\rm dry}(\mathrm{EP_E} + \gamma_{\rm DNA} \ \mathrm{P_{DNA}})} \ . \label{eq:QP}$$

We treat concentrations of bioavailable nitrogen and phosphate as latent variables, modeled using the gene frequencies for nitrogen and phosphate uptake genes in *Prochlorococcus and Synechococcus*, respectively.

$$\log[\mathrm{N_{model}}] = \log[\mathrm{N_0}] - c_\mathrm{N} \mathrm{N_{gene}}, \ \log[\mathrm{P_{model}}] = \log[\mathrm{P_0}] - c_\mathrm{P} \mathrm{P_{gene}}.$$

The terms N_0 , P_0 , c_N , and c_P are model parameters, and N_{gene} and P_{gene} are the gene indices introduced earlier. The diffusion coefficients (D_N , D_P) decrease with temperature using $Q_{10D} = 1.5$. ATOM-gene then finds the trait combination with the largest μ . At the optimal solution either:

$$\mu_E = \mu_L = \mu_N < \mu_P$$
 (N-limitation),
 $\mu_E = \mu_L = \mu_P < \mu_N$ (P-limitation),
 $\mu_E = \mu_L = \mu_P = \mu_N$ (Co-limitation).

ATOM-gene subsequently determines C:P from this optimal strategy. If the strategy is N-limited, then we assume that the cell does luxury P-storage proportional to the modeled P-concentration:

$$P_{\text{stor}} = C_{\text{stor}}[P_{\text{model}}] \max(0, \mu_{c} - \mu),$$

where μ_C is a growth rate cutoff above which luxury storage stops.

We selected a prior probability distribution over model parameters (Supplementary Table 2) and implemented ATOM-Gene within the STAN probabilistic programming language (Carpenter et. al.). We integrated C:P, N and P gene indices, temperature, and irradiance (averaged over the top 50 meters), and calculated the posterior probability distribution over model parameters assuming a log-normal probability distribution for C:P:

$$(C:P)_{obs} \sim lognormal((C:P)_{Atom-gene}(I,T,N_{gene},P_{gene},\sigma)).$$

We performed this Bayesian optimization for the gene indices computed from both Prochlorococcus and Synechococcus leading to a statistical model of C:P.

Galbraith-Martiny and P-Regression Model

The Galbraith-Martiny model [43] calculates P:C as a linear function of phosphate concentration:

$$(P:C)_{GM} = 6.9x10^{3}[P_{obs}] + 6.0x10^{-3}.$$

We also created a P-regression based model (Preg) by refitting the Galbraith-Martiny GM model just to the data-set gathered here, assuming a lognormal error model:

$$(P:C)_{Preg} \sim lognormal(\kappa[P_{obs}] + [P_0], \sigma).$$

Yvon-Durocher Model and T-Regression Model

The Yvon-Durocher model [44] expresses phytoplankton C:P as an exponential function of temperature: $\log (C:P)_{YD} = \Pi(T-15) + b$,

where $\Pi = 0.037^{\circ}\text{C}^{-1}$ and b = 5.010. We also created a T-Regression based model by refitting the Yvon-Durocher model to the data-set gathered here, assuming lognormal errors:

$$(C:P)_{Treg} \sim lognormal(\Pi(T-15) + b, \sigma).$$

Moreno-Hagstrom Model

The Moreno-Hagstrom model [42] uses the radius (r) and allocation of biomass to biosynthesis (E) and photosynthesis (L) to model C:P, by calculating the trait-combination that leads to maximal growth for each combination of irradiance (I), temperature (T), and phosphorus (P). The Moreno-Hagstrom model models luxury-P storage as a linear function of P, so that:

$$(\text{C:P})_{\text{MH}} = \frac{1}{\left((\text{C:P})_{\text{structure}} + f_{\text{storage}}[P_{\text{obs}}]\right)}.$$

It should be noted the relationship between polyphosphate storage and ambient P concentrations has been demonstrated to have an inverse relationship in subtropical North Atlantic *Synechococcus* [45], but the direction appears to be regional dependent [46].

Results

We quantified the variation in the Carbon-to-Phosphorus (C:P) elemental stoichiometry across ocean environmental gradients in the Atlantic, Indian and Pacific Ocean (Figure 1). Generally, C:P ratios decreased towards colder water and higher nutrient concentrations. This pattern was present in the temperate region in the North Atlantic (Figure 1A) and equatorial upwelling in the Pacific Ocean. (Figure 1B). However, in the Indian Ocean C:P decreased toward lower phosphate concentrations and warmer water (Figure 1C) and thus showed the opposite relationship to temperature [3]. Statistical models based solely on phosphate (G-M) or temperature (Y-D) were unable to capture the C:P trends in the Indian Ocean and showed significant biases (Figure 2). All models overestimated C:P in large parts of the Indian Ocean and either over- or underestimated C:P in the equatorial Pacific Ocean. This bias remained even if we refitted the G-M and Y-D models observations from this study suggesting a structural bias. We next tested a more complex previously published trait-based model (Moreno et al), but this model had strong bias, too. Thus, existing models driven by common abiotic factors were unable to predict shifts in the elemental stoichiometry of marine communities.

The incorporation of genomically-derived resource acquisition traits into our model greatly improved the prediction of regional shifts in elemental stoichiometry (Figure 2, R = 0.51 for ATOM-Syn. gene, R = 0.26 for ATOM-Pro. gene). The models incorporating genomically derived traits remained superior in a comparison based on information criteria computed using cross-validation [47] (Supplemental Table 7). We derived resource acquisition traits in *Prochlorococcus* and *Synechococcus* (the two most abundant phytoplankton in these samples) [26] from metagenomes. We then used relative gene frequency of nitrogen and phosphorus acquisition genes to develop an index for the induction of nutrient acquisition machinery for each nutrient and lineage (Supplementary Figure 4). This index assumes cyanobacterial lineages adapt to their environment through genome streamlining and the presence or absence of nutrient acquisition genes are directly related to nutrient stress. We found that shifts in adaptation and investment strategies for nutrient uptake led to lower bias in all the regions (Figure 1, Figure 5). For example, this was the only model that captured the latitudinal gradient in C:P in the Indian Ocean (Figure 1). ATOM-gene is a nonlinear model, and predicted elevated C:P when either the N or P gene index is close to the max. The difference between the North Atlantic Subtropical Gyre and the North Indian is that the gene indices diverge more in the Subtropical North Atlantic. The P gene index is notably higher in the Subtropical North Atlantic than the North Indian. Thus, the nutrient limitation is more extreme in the Subtropical North Atlantic, compared with the North Indian. Similarly, the South Indian has higher C:P because the N gene index peaks there (and the same is true in a few North Pacific data points). Thus, the ATOM-gene model was able to incorporate a previously unknown pattern of nutrient gene frequencies to predict the regional shifts in C:P.

The frequency of nutrient acquisition genes helped resolve variation in nutrient stress at very low nutrient concentrations. We observed a significant correlation between shifts in nutrient acquisition gene frequencies and the ambient nutrient concentration (Figure 3). This was seen for both phosphorus and nitrogen acquisition genes and their respective inorganic nutrient concentrations. However, the ambient nutrient concentration of phosphorus and especially nitrogen was below detection limit in many samples. Additionally, we observed higher relative gene frequencies for iron in the Subtropical Indian Ocean, Equatorial Pacific, and the North Atlantic in *Prochlorococcus* metagenomes (Figure 4a). Whereas higher iron stress in Indian Ocean overlaps with low macronutrient availability, high macronutrient availability is typical of the Equatorial Pacific and Temperate North Atlantic, as shown by N and P relative gene frequencies (Figure 4). Here we detected large variations in gene frequencies suggesting corresponding shifts in nutrient stress. Thus, metagenomic analyses across diverse ocean regions provided a high-sensitivity quantification of nutrient stress.

The frequency of *Prochlorococcus* acquisition genes suggested regional shifts in nutrient stress by both a single and multiple nutrients. As seen in earlier studies, we detected a high frequency of P acquisition genes for *Prochlorococcus* in the subtropical North Atlantic Ocean below 39°N, where phosphate concentrations were low (Figure 4A)[41]. This included genes responsible for the regulation and uptake of dissolved organic P, arsenate detoxification, and several of unknown function. We also saw elevated P acquisition genes for *Prochlorococcus* in the north Indian Ocean and Bay of Bengal (between 1° and 17°N). In contrast, P acquisition genes were low in all samples from the Pacific Ocean and south Indian Ocean. *Prochlorococcus* N acquisition genes showed a different biogeographical pattern. Urea acquisition genes were frequent in all samples with the exception of the high nitrate areas in the equatorial Pacific Ocean and temperate waters in the North Atlantic Ocean. Nitrite and nitrate acquisition genes were frequent throughout the Indian Ocean (with the exception of samples on the equator) and in the northern part of the Pacific Ocean transect. However, nitrite and nitrate genes were less common in the North Atlantic subtropical waters. Iron acquisition genes were common in equatorial Pacific Ocean. Thus, we detected a clear biogeography of genes involved in N, P, and Fe in *Prochlorococcus*.

We observed a partial correspondence between the frequency of nutrient acquisition genes in *Prochlorococcus* and *Synechococcus* suggesting some lineage-specific adaptations to specific ocean environmental conditions (Figure 4A). Overall, the regional shifts in *Prochlorococcus* and *Synechococcus* genome content were significantly correlated (Mantel test R = 0.65, *p*-value < 0.001). In *Synechococcus*, there was also a high frequency of P acquisition genes in the subtropical North Atlantic Ocean and north Indian Ocean (Figure 4C). However, it appeared that the Indian Ocean area with high P acquisition genes spread further south in *Synechococcus* compared to *Prochlorococcus*. N acquisition genes were also frequent in nearly all samples for *Synechococcus*, whereas the genes were more geographically restricted in *Prochlorococcus*. There was some evidence of increase in *Synechococcus* iron acquisition genes in the equatorial Pacific Ocean, but the pattern was not strong. This method is favorable within the relatively stable environments inhabited by *Synechococcus* and *Prochlorococcus* leading to the selection for specialized ecotypes. The gene index results are more distinct for *Prochlorococcus* (Figure 4), likely due to their higher degree of genomic streamlining. Thus, the biogeographical shifts in nutrient acquisition genes were more pronounced for *Prochlorococcus* compared to *Synechococcus*.

The variation in nutrient acquisition genes may be linked to shifts in stress by one or more nutrients (Figure 4b,d; Supplementary Figure 4). The frequency of nutrient acquisition genes suggested P stress but also some N co-stress in the western North Atlantic Ocean and north Indian Ocean. The North Pacific Ocean and south Indian Ocean appeared to be N stressed. The equatorial Pacific Ocean was iron stressed. However, the gene frequencies suggested that a brief transition region around 10°N in the North Pacific Ocean experienced co-stress by N and Fe. *Synechococcus* appeared to be stressed by N in temperate North Atlantic Ocean waters whereas *Prochlorococcus* appeared more stressed by iron. Similarly, *Synechococcus* showed evidence of P stress in parts of the south Indian Ocean but this was not seen in *Prochlorococcus*. Shifts in the relative gene frequency corresponded to shifts in clade ecotypes (Supplementary Figure 2). Thus, metagenomic analyses of phytoplankton populations suggested regional shifts in stress by one or multiple nutrients.

We used additional ecosystem measurements to verify the predictions from ATOM-gene and the overall resource investment strategies. In the Indian Ocean, uptake kinetics for the ATOM-Gene model were positively correlated with observed uptake rates for nitrate, ammonium, and urea (Figure 5, Supplementary Table 3). The implied nutrient distributions matched our observations of increasing N northwards and vice versa for P into the subtropical Indian Ocean gyre. Increases in N and P uptake rates, cellular investment in photosynthesis and biosynthesis, and cell volume corresponded to reduced nitrogen stress (Supplementary Table 3). The aforementioned parameters were significantly correlated to higher in situ N uptake rates and lower relative N gene frequency for Prochlorococcus and Synechococcus. Phosphorus stress appeared to have little impact on C:P and cellular uptake traits in the Indian Ocean, unlike the other two basins (Supplementary Figure 5). Although P investment increased into the subtropical Indian Ocean gyre, there was little influence on P luxury uptake and storage (Supplementary Figure 10). Supplementary Figures 8 and 9 show draws from the posterior-predictive distribution of C:P. We give summaries of the posterior distribution over model parameters in Supplementary Tables 8 and 9, where $\hat{R} = 1$ suggests convergence of the Markov Chain Monte Carlo integrator. Supplementary Figures 6 and 7 show the posterior draws for each pair of variables. Only larger cells in the temperate North Atlantic exhibited P storage in the ATOM-Gene model. The small

number of data points with metagenome information prevented tight inference of parameter values, but the posterior distribution favors the hypothesis that the effect of nutrient stress on cell size and ribosomal content is the strongest driver of C:P in the regions sampled, with smaller than expected roles for temperature and luxury storage. This is reflected by the posterior favoring small values of the luxury storage parameter and higher values of the Q10 for photosynthetic processes. Consequently, the interaction between N and P stress as seen in the genomic observations could be the underlying mechanism leading to latitudinal shifts in C:P.

Discussion

Linking 'omics with global biogeochemistry is a major research challenge and opportunity [48–51]. A great deal of molecular data is being generated [52,53], but there is a limited current application of this new knowledge towards understanding large-scale changes in the Earth system [54]. Trait-based approaches are attractive for scaling from individual organisms to key ecosystem functions by using a model intermediate [55,56]. We here use this approach as an intermediate for linking genomic information with ocean biogeochemical processes. By quantifying the spatial variation due to differences in nutrient assimilation genes, we improved our predictions of C:P across three major ocean basins (Figure 1 and 2). The ATOM-gene model allowed for multiple nutrient indexes (N and P), where *in situ* nutrient observations were undetectable, resulting in significant improvements to the existing trait model [42]. Importantly, the gene index quantifies cyanobacterial adaptation to nutrient stressors in regions for which we have limited knowledge (e.g., the central Indian Ocean). Nutrient stress may occur through diffusive limitation at low ambient concentrations, the magnitude of nutrient fluxes, the ratio of nutrient supply, or nutrient co-limitation. Additionally, both *Synechococcus* and *Prochlorococcus* can utilize different P and N sources [57]. Thus, genome shifts integrate these unknowns through the selective pressure to retain particular genes in nutrient-poor biomes.

The frequency of nutrient assimilation genes greatly improved our understanding of nutrient stress and elemental stoichiometry of marine communities. In particular, the results showed surprising patterns of P and N stress in the less studied Indian Ocean. Our results support a recent analysis of *Synechococcus* and *Prochlorococcus* elemental quotas, leading to a gradient of N, P, and Fe stress in the Indian Ocean [58]. The Bay of Bengal showed evidence of P stress but lower N:P and C:P ratios. We attribute this contradictory observation to an interaction between N and P stress as the upregulation of P uptake proteins is restricted by N stress [59]. Culture studies have shown that N and P stress interact in controlling the overall cellular physiology and C:N:P [5]. However, it has been a challenge to translate these findings to field communities. Some of this confusion originates from difficulties in constraining external N and possibly P sources from atmospheric deposition and N-fixation. This leads to a poorly constrained N:P supply ratio. It is unclear why we see evidence of increased P stress near the Bay of Bengal, but it is tempting to attribute it to elevated N-fixation [8,60]. Similar to recent observations of dissolved and particulate Fe, we saw indications of Fe stress via *Prochlorococcus* Fe assimilation genes in the Subtropical Indian Ocean gyre [58,61]. We also saw a high presence of Fe assimilation genes in regions with low C:P, where Synechococcus and Prochlorococcus cell abundances remained elevated [28]. As expected, this was seen for the equatorial Pacific HNLC region [62]. Our data also support past studies indicating that the subtropical North Atlantic Ocean [63] and the southern Indian Ocean [58] could experience some iron stress. Thus, our genomic techniques are unveiling regions, where we have a limited understanding of trace-metal stress.

Our approach is based on an assumption of rapid adaptation leading to direct association between genome content and environmental conditions [64–67]. Tropical and subtropical ocean regions have fast bacterial turnover leading to rapid selection and genome streamlining [68]. However, environments with slow bacterial turnover may include ecotypes or genes that reflect past environmental conditions. Different lineages may also experience unique stress [69] whereas we here only analyzed the abundant marine Cyanobacteria. Our dataset includes few representative stations from high latitudes, where light or temperature may be the dominant selective factors [70,71]. In such conditions, transcriptomics or proteomics may be more applicable. However, these techniques suffer from their own caveats like strong diel cycles [72,73] or low correlation between RNA and protein expression [74,75]. Thus, the exact link between 'omics measurements and biogeochemical processes needs to be tailored to the system of interest.

'Omics techniques can be powerful for understanding the environmental conditions experienced by microorganisms. This principle is also applied in other ecosystem settings. A high presence of Proteobacteria in the human gut may be an indicator of an imbalance in the redox potential and 'ecosystem' dysbiosis [76]. Similarly, the presence of ammonia monooxygenase may be indicative of nitrification [77]. In many ecosystems, it can be very challenging to quantify microbial physiology and stress. Thus, a carefully calibrated genomic approach could become a widespread tool for understand microbial responses to environmental changes and the biogeochemical outcomes.

Acknowledgments

We would like to thank Jim Prosser and Jennifer Martiny for organizing this special issue and the National Science Foundation (NSF) (OCE-1559002, OCE-1848576, OCE-1756054) the National Aeronautics and Space Administration Earth and Space Science Fellowship (NESSF16R) and NIH T32AI141346 for supporting this work. GIH acknowledges the support of NSF grant OCE-1848576 and Simons Foundation Grant Number: 395890. We would like to thank Claudia Weihe for guidance in preparing metagenome libraries, and the scientists and crews aboard the NH1418, AE1319, BV46, and I09 cruises for their effort.

Figures and Tables

Table 1: Mean environmental characteristics for each ocean cruise transect. Pro = Prochlorococcus, Syn = Synechococcus, Pmax = maximum uptake rate, Ks = half saturation PO₄ concentration. BD = below detection and NA = not measured. Pmax (maximum uptake of PO₄) and Ks (half saturation concentration of PO₄) are calculated according to Micheaelis-Menton functional kinetics for the whole community [25]; Puptake₄ = (Pmax * [P₁]) / ([P₁] + Ks).

Figure 1: Observations and predictions of seston elemental stoichiometry. *In situ* measurements of particulate organic matter C:P are shown in gray, with selected stations in black where nutrient uptake incubations were performed for the *(a)* Atlantic *(b)* Pacific and *(c)* Indian Oceans [3]. Predicted C:P is shown by the ATOM-Syn trait-gene model (blue) and Galbraith-Martiny [43] phosphate regression model (red). Additional environmental variables of temperature (green), photosynthetically active radiation (purple), and phosphate (orange) are shown below for the *(d)* Atlantic *(e)* Pacific and *(f)* Indian Oceans from Supplementary Table 2.

Figure 2. Trait model C:P bias. Statistical results for the predicted C:P models showing (a) Coefficient of determination (b) residuals (log_w (predictions) – log_w (observations)) across stations where surface C:P measurements were taken. Red indicates a positive bias, and blue negative bias. Since the distribution of C:P data looks much more lognormal we plotted the bias of the log-transformed data and models, and computed the percentage of variance of the log-transformed data that the models explained. The coefficient of determination was calculated as;

 $R^2 = 1 - [\text{mean}(\log_{10}(\text{observations}) - \log_{10}(\text{predictions}))^2) / (\text{mean}((\log_{10}(\text{observations}) - \text{mean}(\log_{10}(\text{observations}))^2))].$

Figure 3. PCA component 1 versus nutrient concentrations. *In situ* nutrient concentrations for phosphate and nitrate are plotted against the first principle component calculated from relative gene frequencies for *(a) Prochlorococcus* phosphorus assimilation genes ($R^2 = 0.65$, p-value < 0.001), *(b) Synechococcus* phosphorus assimilation genes ($R^2 = 0.52$, p-value < 0.001), *(c) Prochlorococcus* nitrogen assimilation genes ($R^2 = 0.78$, p-value < 0.001), and *(d) Synechococcus* nitrogen assimilation genes ($R^2 = 0.02$, p-value = 0.35). High sensitivity phosphate measurements (filled red) were done using a MAGIC-SRP assay [32]. Otherwise nitrate and phosphate observations were taken using standard methods (open circles)[78]. DL = Detection limit.

Figure 4. Variation among relative gene frequencies between stations. Green = nitrogen, Purple = phosphorus, red = iron. Matrices based on normalized gene frequency are significantly correlated (Mantel test R = 0.65, *p*-value < 0.001). The heatmaps for *(a) Prochlorococcus* and *c) Synechococcus* cluster the relative gene frequencies along the top according to functional role for each station row. The Principle Component Analysis (PCA) plots for *(b) Prochlorococcus* and *(d) Synechococcus* show the variation among stations that is solely attributed to differences in relative gene frequencies. If the overall contribution of N, P, or Fe genes cluster along one direction, we have added a textbox labeled "N stress, P

stress, or Fe Stress" to panels (*b*) and (*d*). *Prochlorococcus* relative gene frequencies cluster the stations according to these three nutrient stressors. *Synechococcus* relative gene frequencies cluster the stations mainly along two (Fe and P stress), with weak contributions from N relative gene frequencies. A red asterisk (*) has been added to samples deeper than 50m.

Figure 5. Evaluation of nutrient stress indices against ATOM-Gene and *in situ* uptake parameters in the Indian Ocean. Relative gene frequencies of (a) nitrogen and (b) phosphorus genes is shown for *Prochlorococcus* (blue) and *Synechococcus* (orange-red). ATOM-Gene estimates for (c) N uptake and (d) P uptake normalized to cell volume are compared to the *in situ* parameters of (e) Absolute uptake of N species (nitrate-green, urea-purple ammonium-gold) and (f) the ratio of particulate organic carbon to phosphorus. *In situ* uptake rates and C:P are presented in [3,26]. Absolute uptake rates measure the accumulation of a substrate within particles.

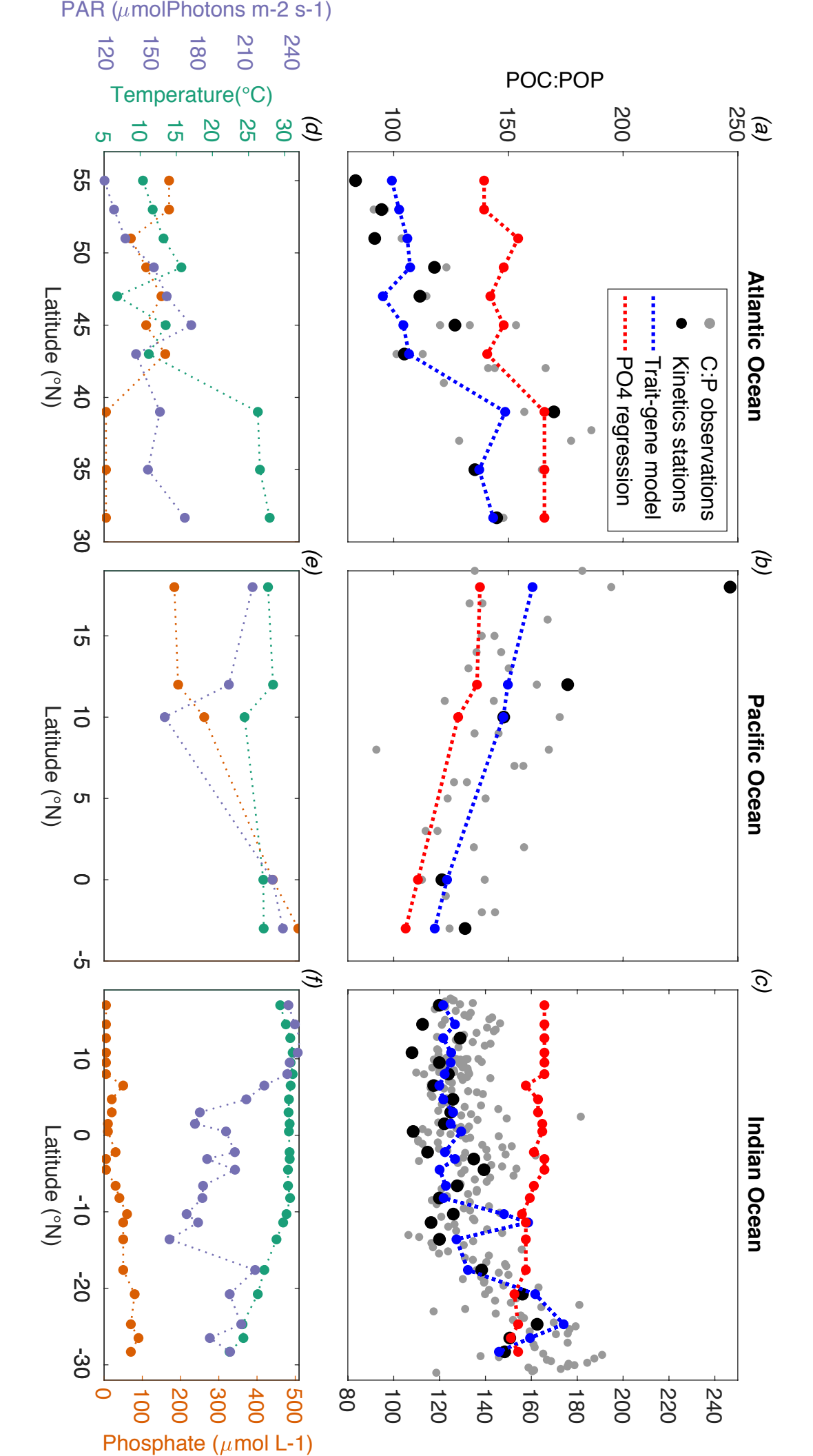
References

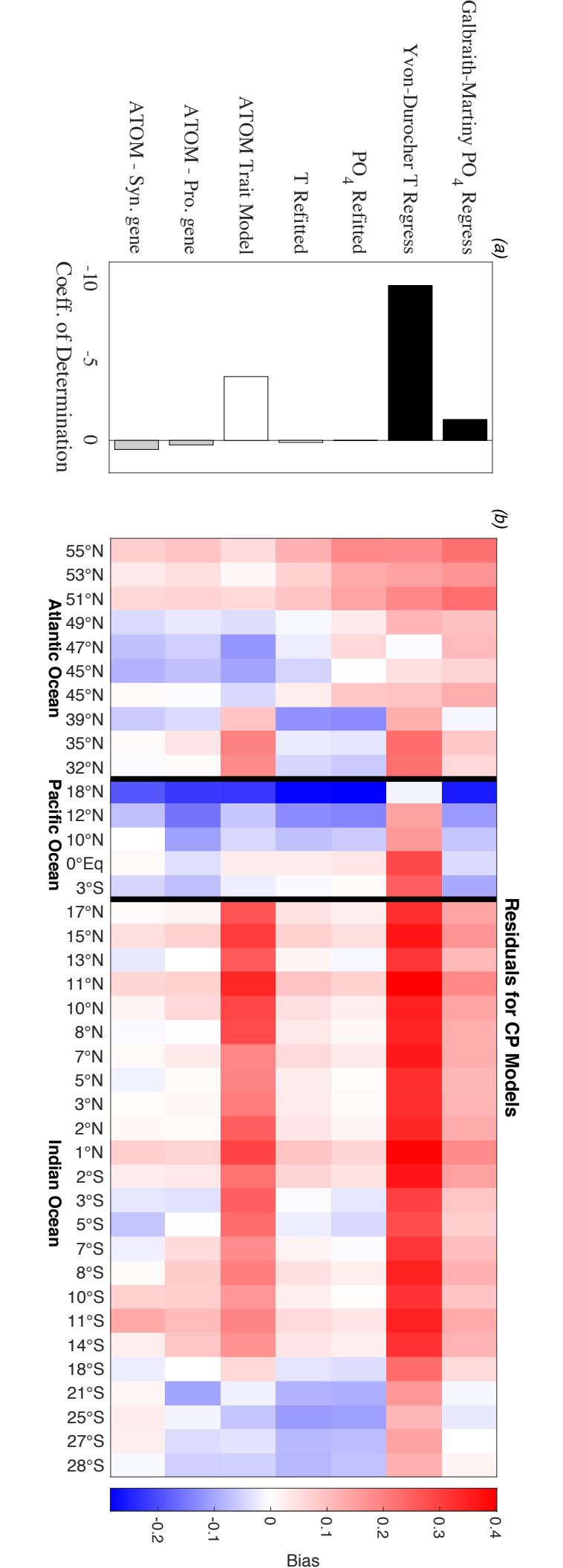
- 1. Sterner RW, Elser JJ. 2002 *Ecological Stoichiometry: The Biology of Elements from Molecules to the Biosphere.* Princeton University Press. See http://books.google.com/books?hl=en&lr=&id=53NTDvppdYUC&pgis=1.
- 2. Moreno AR, Martiny AC. 2018 Ecological Stoichiometry of Ocean Plankton. *Ann. Rev. Mar. Sci.* **10**, 1–27. (doi:10.1146/annurev-marine-121916-063126)
- 3. Garcia CA, Baer SE, Garcia NS, Rauschenberg S, Twining BS, Lomas MW, Martiny AC. 2018 Nutrient supply controls particulate elemental concentrations and ratios in the low latitude eastern Indian Ocean. *Nat. Commun.* **9**, 4868. (doi:10.1038/s41467-018-06892-w)
- 4. MONOD J. 1950 Technique, Theory and Applications of Continuous Culture. *Ann. Inst. Pasteur* **79**, 390–410.
- 5. Klausmeier CA, Litchman E, Levin SA. 2004 Phytoplankton growth and stoichiometry under multiple nutrient limitation. *Limnol. Oceanogr.* **49**, 1463–1470. (doi:10.4319/lo.2004.49.4_part_2.1463)
- 6. Martiny AC, Pham CTA, Primeau FW, Vrugt JA, Moore JK, Levin SA, Lomas MW. 2013 Strong latitudinal patterns in the elemental ratios of marine plankton and organic matter. *Nat. Geosci.* **6**, 279–283. (doi:10.1038/ngeo1757)
- 7. Alexander H, Jenkins BD, Rynearson TA, Dyhrman ST. 2015 Metatranscriptome analyses indicate resource partitioning between diatoms in the field. *Proc. Natl. Acad. Sci. U. S. A.* **112**, E2182–E2190. (doi:10.1073/pnas.1421993112)
- 8. Martiny AC *et al.* 2019 Biogeochemical controls of surface ocean phosphate. *Sci. Adv.* **5**, eaax0341. (doi:10.1126/sciadv.aax0341)
- 9. Shilova IN *et al.* 2017 Differential effects of nitrate, ammonium, and urea as N sources for microbial communities in the North Pacific Ocean. *Limnol. Oceanogr.* **62**, 2550–2574. (doi:10.1002/LNO.10590@10.1002/(ISSN)1939-5590.ALOHA30)
- 10. Guidot A, Verner MC, Debaud JC, Marmeisse R. 2005 Intraspecific variation in use of different organic nitrogen sources by the ectomycorrhizal fungus Hebeloma cylindrosporum. *Mycorrhiza* **15**, 167–177. (doi:10.1007/s00572-004-0318-1)
- 11. Tapia-Torres Y, Rodríguez-Torres MD, Elser JJ, Islas A, Souza V, García-Oliva F, Olmedo-Álvarez G. 2016 How to live with phosphorus scarcity in soil and sediment: Lessons from bacteria. *Appl. Environ. Microbiol.* **82**, 4652–4662. (doi:10.1128/AEM.00160-16)
- 12. Sosa OA, Casey JR, Karl DM. 2019 Methylphosphonate Oxidation in *Prochlorococcus* Strain MIT9301 Supports Phosphate Acquisition, Formate Excretion, and Carbon Assimilation into Purines. *Appl. Environ. Microbiol.* **85**. (doi:10.1128/AEM.00289-19)
- 13. Herrero A, Muro-Pastor AM, Flores E. 2001 Nitrogen control in cyanobacteria. *J. Bacteriol.* **183**, 411–425. (doi:10.1128/JB.183.2.411-425.2001)
- 14. Bonachela JA, Allison SD, Martiny AC, Levin SA. 2013 A model for variable phytoplankton stoichiometry based on cell protein regulation. *Biogeosciences* **10**, 4341–4356. (doi:10.5194/bg-10-4341-2013)
- 15. Zimmerman AE, Allison SD, Martiny AC. 2014 Phylogenetic constraints on elemental stoichiometry and resource allocation in heterotrophic marine bacteria. *Environ. Microbiol.* **16**, 1398–1410. (doi:10.1111/1462-2920.12329)
- 16. Martiny JBH, Jones SE, Lennon JT, Martiny AC. 2015 Microbiomes in light of traits: A

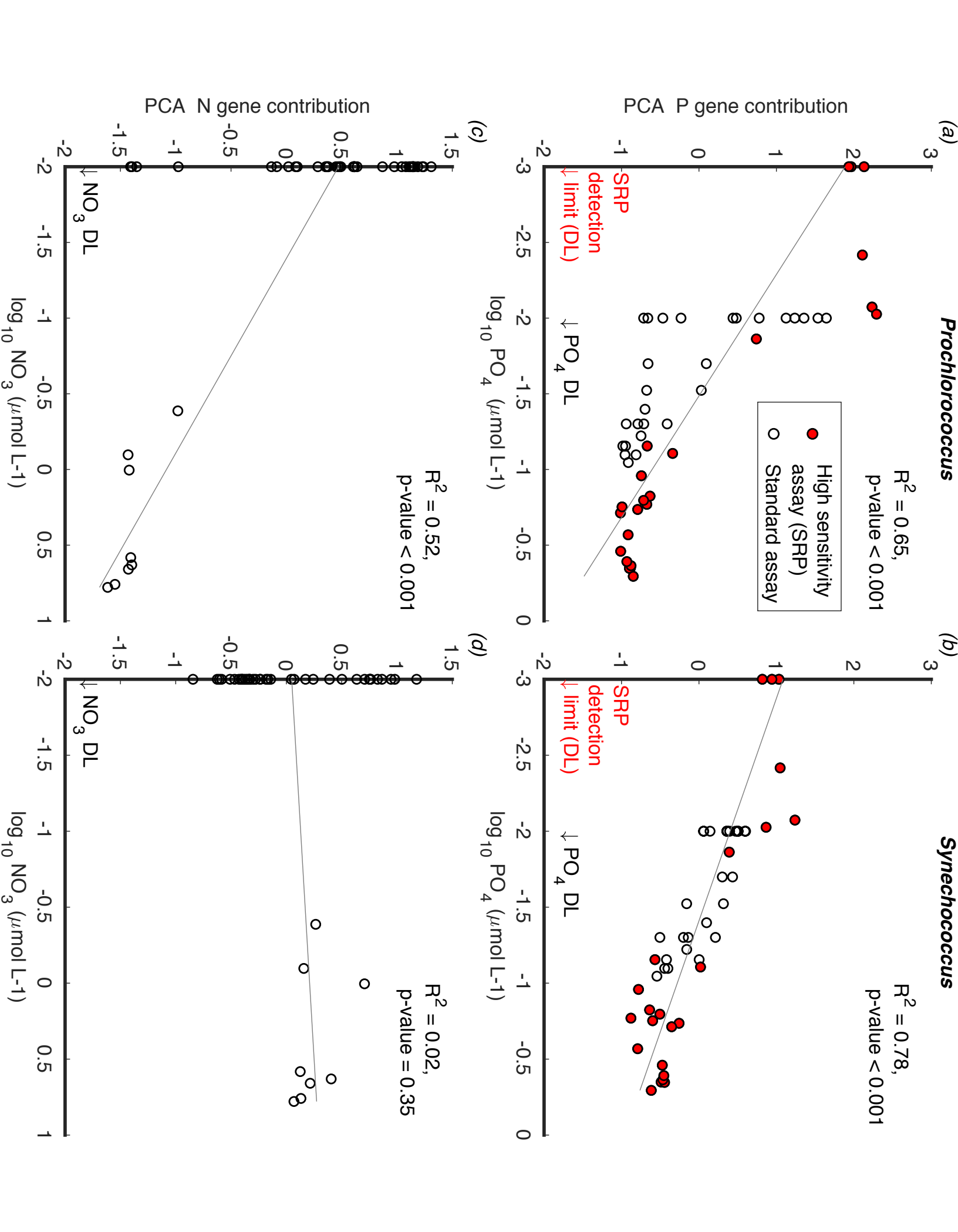
- phylogenetic perspective. Science (80-.). 350. (doi:10.1126/science.aac9323)
- 17. Scanlan DJ *et al.* 2009 Ecological Genomics of Marine Picocyanobacteria. *Microbiol. Mol. Biol. Rev.* **73**, 249–299. (doi:10.1128/mmbr.00035-08)
- 18. Morris JJ, Lenski RE, Zinser ER. 2012 The Black Queen Hypothesis: evolution of dependencies through adaptive gene loss. *MBio* **3**, e00036-12-. (doi:10.1128/mBio.00036-12)
- 19. Martiny AC, Coleman ML, Chisholm SW. 2006 Phosphate acquisition genes in Prochlorococcus ecotypes: Evidence for genome-wide adaptation. *Proc. Natl. Acad. Sci.* **103**, 12552–12557. (doi:10.1073/pnas.0601301103)
- 20. Coleman ML, Chisholm SW. 2010 Ecosystem-specific selection pressures revealed through comparative population genomics. *Proc. Natl. Acad. Sci. U. S. A.* **107**, 18634–18639. (doi:10.1073/pnas.1009480107)
- 21. Martiny AC, Huang Y, Li W. 2009 Occurrence of phosphate acquisition genes in Prochlorococcus cells from different ocean regions. *Environ. Microbiol.* **11**, 1340–1347. (doi:10.1111/j.1462-2920.2009.01860.x)
- 22. Antelmann H, Scharf C, Hecker M. 2000 Phosphate starvation-inducible proteins of Bacillus subtilis: Proteomics and transcriptional analysis. *J. Bacteriol.* **182**, 4478–4490. (doi:10.1128/JB.182.16.4478-4490.2000)
- 23. Martiny AC, Kathuria S, Berube PM. 2009 Widespread metabolic potential for nitrite and nitrate assimilation among Prochlorococcus ecotypes. *Proc. Natl. Acad. Sci. U. S. A.* **106**, 10787–10792. (doi:10.1073/pnas.0902532106)
- 24. Berube PM *et al.* 2015 Physiology and evolution of nitrate acquisition in Prochlorococcus. *ISME J.* **9**, 1195–1207. (doi:10.1038/ismej.2014.211)
- 25. Lomas MW, Bonachela JA, Levin SA, Martiny AC. 2014 Impact of ocean phytoplankton diversity on phosphate uptake. *Proc. Natl. Acad. Sci.* **111**, 17540–17545. (doi:10.1073/pnas.1420760111)
- 26. Baer SE, Rauschenberg S, Garcia CA, Garcia NS, Martiny AC, Twining BS, Lomas MW. 2018 Carbon and nitrogen productivity during spring in the oligotrophic Indian Ocean along the GO-SHIP IO9N transect. *Deep Sea Res. Part II Top. Stud. Oceanogr.* (doi:10.1016/J.DSR2.2018.11.008)
- 27. Baer SE, Lomas MW, Terpis KX, Mouginot C, Martiny AC. 2017 Stoichiometry of Prochlorococcus, Synechococcus, and small eukaryotic populations in the western North Atlantic Ocean. *Environ. Microbiol.* **19**, 1568–1583. (doi:10.1111/1462-2920.13672)
- 28. Kent AG, Baer SE, Mouginot C, Huang JS, Larkin AA, Lomas MW, Martiny AC. 2019 Parallel phylogeography of Prochlorococcus and Synechococcus. *ISME J.* **13**, 430–441. (doi:10.1038/s41396-018-0287-6)
- 29. Larkin AA, Garcia CA, Ingoglia KA, Garcia NS, Baer SE, Twining BS, Lomas MW, Martiny AC. 2019 Subtle biogeochemical regimes in the Indian Ocean revealed by spatial and diel frequency of Prochlorococcus haplotypes . *Limnol. Oceanogr.* (doi:10.1002/lno.11251)
- 30. Steinberg DK, Carlson CA, Bates NR, Johnson RJ, Michaels AF, Knap AH. 2001 Overview of the US JGOFS Bermuda Atlantic Time-series Study (BATS): A decade-scale look at ocean biology and biogeochemistry. *Deep. Res. Part II Top. Stud. Oceanogr.* **48**, 1405–1447. (doi:10.1016/S0967-0645(00)00148-X)
- 31. Lomas MW, Burke AL, Lomas DA, Bell DW, Shen C, Dyhrman ST, Ammerman JW. 2010 Sargasso Sea phosphorus biogeochemistry: an important role for dissolved organic phosphorus (DOP). *Biogeosciences* **7**, 695–710. (doi:10.5194/bg-7-695-2010)
- 32. Karl DM, Tien G. 1992 MAGIC: A sensitive and precise method for measuring dissolved phosphorus in aquatic environments. *Limnol. Oceanogr.* **37**, 105–116. (doi:10.4319/lo.1992.37.1.0105)
- 33. Larkin AA, Martiny AC. 2017 Microdiversity shapes the traits, niche space, and biogeography of microbial taxa. *Environ. Microbiol. Rep.* **9**, 55–70. (doi:10.1111/1758-2229.12523)
- 34. Boström KH, Simu K, Hagström Å, Riemann L. 2004 Optimization of DNA extraction for quantitative marine bacterioplankton community analysis. *Limnol. Oceanogr. Methods* **2**, 365–373. (doi:10.4319/lom.2004.2.365)
- 35. Bolger AM, Lohse M, Usadel B. 2014 Trimmomatic: A flexible trimmer for Illumina sequence data. *Bioinformatics* **30**, 2114–2120. (doi:10.1093/bioinformatics/btu170)
- 36. Langmead B, Salzberg SL. 2012 Fast gapped-read alignment with Bowtie 2. *Nat. Methods* **9**, 357–359. (doi:10.1038/nmeth.1923)
- 37. Eren AM, Esen OC, Quince C, Vineis JH, Morrison HG, Sogin ML, Delmont TO. 2015 Anvi'o: An advanced analysis and visualization platformfor 'omics data. *PeerJ* **2015**. (doi:10.7717/peerj.1319)
- 38. Buchfink B, Xie C, Huson DH. 2014 Fast and sensitive protein alignment using DIAMOND. Nat.

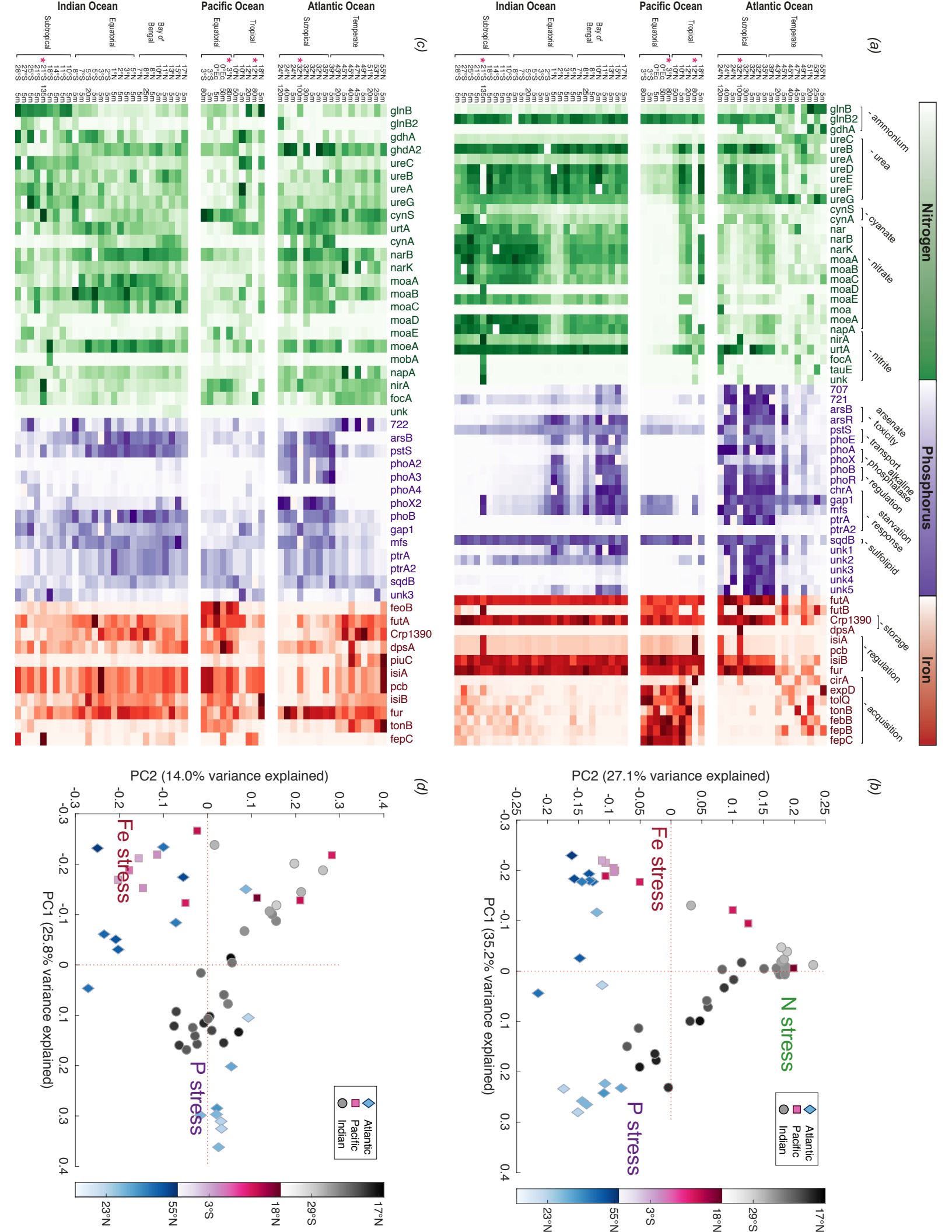
- Methods. 12, 59–60. (doi:10.1038/nmeth.3176)
- 39. Malmstrom RR *et al.* 2013 Ecology of uncultured Prochlorococcus clades revealed through single-cell genomics and biogeographic analysis. *ISME J.* 7, 184–198. (doi:10.1038/ismej.2012.89)
- 40. Robidart JC, Magasin JD, Shilova IN, Turk-Kubo KA, Wilson ST, Karl DM, Scholin CA, Zehr JP. 2019 Effects of nutrient enrichment on surface microbial community gene expression in the oligotrophic North Pacific Subtropical Gyre. *ISME J.* **13**, 374–387. (doi:10.1038/s41396-018-0280-0)
- 41. Martiny AC, Ustick L, A. Garcia Č, Lomas MW. 2019 Genomic adaptation of marine phytoplankton populations regulates phosphate uptake. *Limnol. Oceanogr.* (doi:10.1002/lno.11252)
- 42. Moreno AR, Hagstrom GI, Primeau FW, Levin SA, Martiny AC. 2018 Marine phytoplankton stoichiometry mediates nonlinear interactions between nutrient supply, temperature, and atmospheric CO2. *Biogeosciences* (doi:10.5194/bg-15-2761-2018)
- 43. Galbraith ED, Martiny AC. 2015 A simple nutrient-dependence mechanism for predicting the stoichiometry of marine ecosystems. *Proc. Natl. Acad. Sci.* **112**, 8199–8204. (doi:10.1073/pnas.1423917112)
- 44. Yvon-Durocher G, Dossena M, Trimmer M, Woodward G, Allen AP. 2015 Temperature and the biogeography of algal stoichiometry. *Glob. Ecol. Biogeogr.* **24**, 562–570. (doi:10.1111/geb.12280)
- 45. Martin P, Dyhrman ST, Lomas MW, Poulton NJ, Van Mooy BAS. 2014 Accumulation and enhanced cycling of polyphosphate by Sargasso Sea plankton in response to low phosphorus. *Proc. Natl. Acad. Sci. U. S. A.* 111, 8089–8094. (doi:10.1073/pnas.1321719111)
- 46. Li J, Dittrich M. 2019 Dynamic polyphosphate metabolism în cyanobacteria responding to phosphorus availability. *Environ. Microbiol.* **21**, 572–583. (doi:10.1111/1462-2920.14488)
- 47. Vehtari A, Gelman A, Gabry J. 2017 Practical Bayesian model evaluation using leave-one-out cross-validation and WAIC. *Stat. Comput.* **27**, 1413–1432. (doi:10.1007/s11222-016-9696-4)
- 48. Mock T, Daines SJ, Geider R, Collins S, Metodiev M, Millar AJ, Moulton V, Lenton TM. 2016 Bridging the gap between omics and earth system science to better understand how environmental change impacts marine microbes. *Glob. Chang. Biol.* 22, 61–75. (doi:10.1111/gcb.12983)
- 49. Coles VJ *et al.* 2017 Ocean biogeochemistry modeled with emergent trait-based genomics. *Science* (80-.). **358**, 1149–1154. (doi:10.1126/science.aan5712)
- 50. Hennon GMM, Dyhrman ST. 2019 Progress and promise of omics for predicting the impacts of climate change on harmful algal blooms. *Harmful Algae*. (doi:10.1016/j.hal.2019.03.005)
- 51. Caputi L *et al.* 2019 Community-Level Responses to Iron Availability in Open Ocean Plankton Ecosystems. *Global Biogeochem. Cycles* **33**, 391–419. (doi:10.1029/2018GB006022)
- 52. Sunagawa S *et al.* 2015 Structure and function of the global ocean microbiome. *Science* (80-.). **348**. (doi:10.1126/science.1261359)
- 53. Venter JC *et al.* 2004 Environmental Genome Shotgun Sequencing of the Sargasso Sea. *Science* (80-.). **304**, 66–74. (doi:10.1126/science.1093857)
- 54. Moran MA. 2015 The global ocean microbiome. Science (80-.). 350. (doi:10.1126/science.aac8455)
- 55. Kiørboe T, Visser A, Andersen KH. 2018 A trait-based approach to ocean ecology. *ICES J. Mar. Sci.* **75**, 1849–1863. (doi:10.1093/icesjms/fsy090)
- 56. Talmy D, Blackford J, Hardman-Mountford NJ, Dumbrell AJ, Geider RJ. 2013 An optimality model of photoadaptation in contrasting aquatic light regimes. *Limnol. Oceanogr.* **58**, 1802–1818. (doi:10.4319/lo.2013.58.5.1802)
- 57. Moore LR, Post AF, Rocap G, Chisholm SW. 2002 Utilization of different nitrogen sources by the marine cyanobacteria Prochlorococcus and Synechococcus. *Limnol. Oceanogr.* **47**, 989–996. (doi:10.4319/lo.2002.47.4.0989)
- 58. Twining BS, Rauschenberg S, Baer SE, Lomas MW, Martiny AC, Antipova O. 2019 A nutrient limitation mosaic in the eastern tropical Indian Ocean. *Deep. Res. Part II Top. Stud. Oceanogr.* (doi:10.1016/j.dsr2.2019.05.001)
- 59. Bonachela JA, Raghib M, Levin SA. 2011 Dynamic model of flexible phytoplankton nutrient uptake. *Proc. Natl. Acad. Sci.* (doi:10.1073/pnas.1118012108)
- 60. Wang WL, Moore JK, Martiny AC, Primeau FW. 2019 Convergent estimates of marine nitrogen fixation. *Nature* **566**, 205–211. (doi:10.1038/s41586-019-0911-2)
- 61. Grand MM, Measures CI, Hatta M, Hiscock WT, Landing WM, Morton PL, Buck CS, Barrett PM, Resing JA. 2015 Dissolved Fe and Al in the upper 1000 m of the eastern Indian Ocean: A high-resolution transect along 95°E from the Antarctic margin to the Bay of Bengal. *Global Biogeochem. Cycles* **29**, 375–396. (doi:10.1002/2014GB004920)

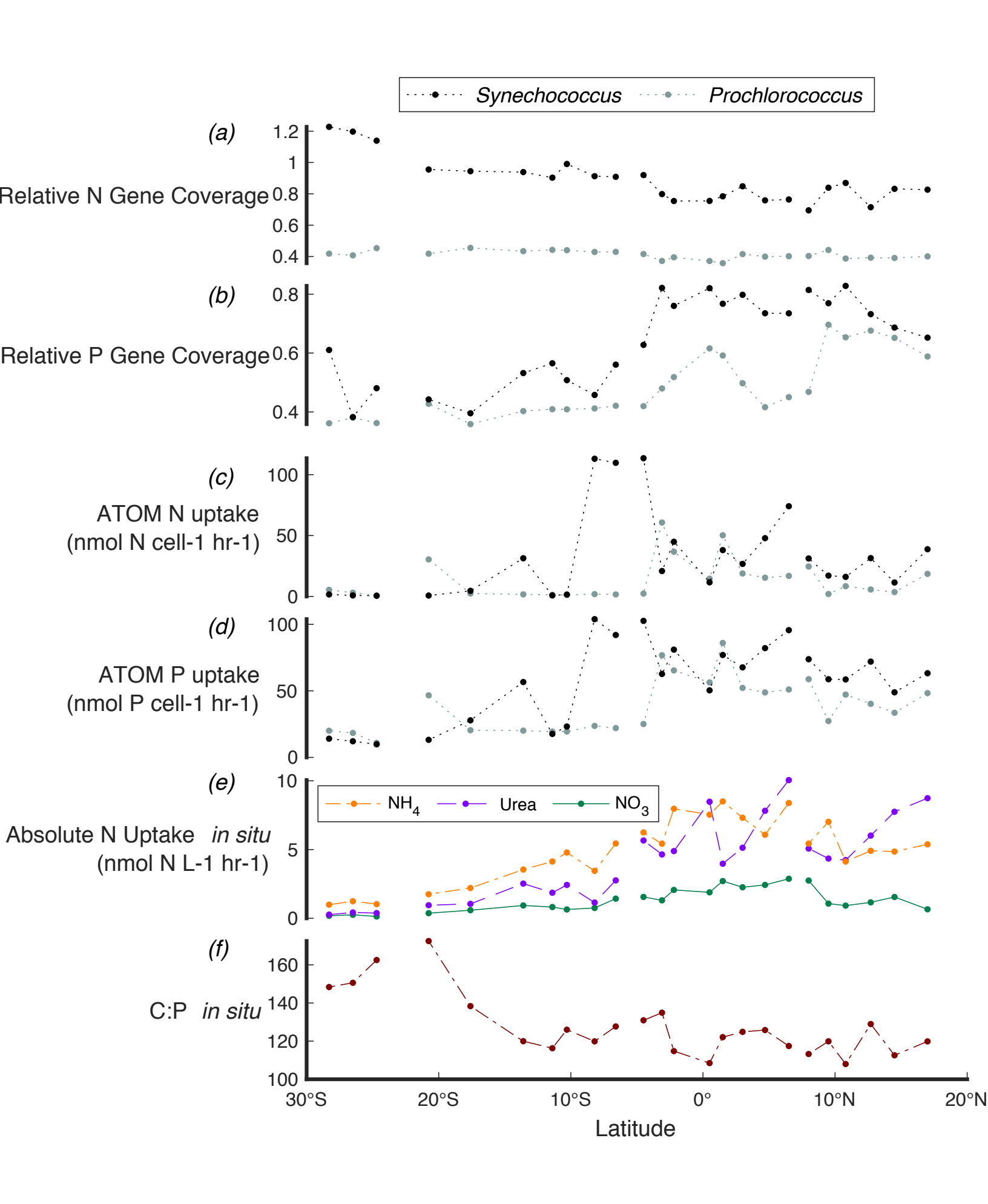
- 62. Coale KH *et al.* 1996 A massive phytoplankton bloom induced by an ecosystem-scale iron fertilization experiment in the equatorial Pacific Ocean. *Nature* **383**, 495. (doi:10.1038/383495a0)
- 63. Rijkenberg MJÂ, Middag R, Laan P, Gerringa LJA, Van Aken HM, Schoemann V, De Jong JTM, De Baar HJW. 2014 The distribution of dissolved iron in the West Atlantic Ocean. *PLoS One* **9**. (doi:10.1371/journal.pone.0101323)
- 64. Partensky F, Garczarek L. 2010 Prochlorococcus: Advantages and Limits of Minimalism. *Ann. Rev. Mar. Sci.* **2**, 305–331. (doi:10.1146/annurev-marine-120308-081034)
- 65. Tripp HJ, Bench SR, Turk KA, Foster RA, Desany BA, Niazi F, Affourtit JP, Zehr JP. 2010 Metabolic streamlining in an open-ocean nitrogen-fixing cyanobacterium. *Nature* **464**, 90–94. (doi:10.1038/nature08786)
- 66. Giovannoni SJ *et al.* 2005 Genetics: Genome streamlining in a cosmopolitan oceanic bacterium. *Science (80-.).* **309**, 1242–1245. (doi:10.1126/science.1114057)
- 67. Swan BK *et al.* 2013 Prevalent genome streamlining and latitudinal divergence of planktonic bacteria in the surface ocean. *Proc. Natl. Acad. Sci. U. S. A.* **110**, 11463–11468. (doi:10.1073/pnas.1304246110)
- 68. Giovannoni SJ, Cameron Thrash J, Temperton B. 2014 Implications of streamlining theory for microbial ecology. *ISME J.* **8**, 1553–1565. (doi:10.1038/ismej.2014.60)
- 69. Alexander H, Rouco M, Haley ST, Wilson ST, Karl DM, Dyhrman ST. 2015 Functional group-specific traits drive phytoplankton dynamics in the oligotrophic ocean. *Proc. Natl. Acad. Sci. U. S. A.* **112**, E5972–E5979. (doi:10.1073/pnas.1518165112)
- 70. Dickman EM, Vanni MJ, Horgan MJ. 2006 Interactive effects of light and nutrients on phytoplankton stoichiometry. *Oecologia* **149**, 676–689. (doi:10.1007/s00442-006-0473-5)
- 71. Thomas MK, Kremer CT, Litchman E. 2016 Environment and evolutionary history determine the global biogeography of phytoplankton temperature traits. *Glob. Ecol. Biogeogr.* **25**, 75–86. (doi:10.1111/geb.12387)
- 72. Poretsky RS, Hewson I, Sun S, Allen AE, Zehr JP, Moran MA. 2009 Comparative day/night metatranscriptomic analysis of microbial communities in the North Pacific subtropical gyre. *Environ. Microbiol.* **11**, 1358–1375. (doi:10.1111/j.1462-2920.2008.01863.x)
- 73. Ottesen EA, Young CR, Gifford SM, Eppley JM, Marin R, Schuster SC, Scholin CA, DeLong EF. 2014 Multispecies diel transcriptional oscillations in open ocean heterotrophic bacterial assemblages. *Science* (80-.). 345, 207–212. (doi:10.1126/science.1252476)
- 74. Jayapal KP, Philp RJ, Kok Y-J, Yap MGS, Sherman DH, Griffin TJ, Hu W-S. 2008 Uncovering genes with divergent mRNA-protein dynamics in Streptomyces coelicolor. *PLoS One* **3**, e2097. (doi:10.1371/journal.pone.0002097)
- 75. Maier T, Schmidt A, Güell M, Kühner S, Gavin AC, Aebersold R, Serrano L. 2011 Quantification of mRNA and protein and integration with protein turnover in a bacterium. *Mol. Syst. Biol.* **7**. (doi:10.1038/msb.2011.38)
- 76. Shin NR, Whon TW, Bae JW. 2015 Proteobacteria: Microbial signature of dysbiosis in gut microbiota. *Trends Biotechnol.* **33**, 496–503. (doi:10.1016/j.tibtech.2015.06.011)
- 77. Francis CA, Roberts KJ, Beman JM, Santoro AE, Oakley BB. 2005 Ubiquity and diversity of ammonia-oxidizing archaea in water columns and sediments of the ocean. *Proc. Natl. Acad. Sci. U. S. A.* **102**, 14683–14688. (doi:10.1073/pnas.0506625102)
- 78. Hood E, Sabine C, Sloyan B. 2016 The GO-SHIP Repeat Hydrography Manual: A collection of expert reports and guidelines. IOCCP Report 14, ICPO Publication Series 134.











Supplementary Information for: Linking regional shifts in microbial genome adaptation with surface ocean biogeochemistry

Authors: Catherine A. Garcia¹, George I. Hagstrom², Alyse Larkin¹, Lucas J. Ustick⁴, Simon A. Levin², Michael W. Lomas³, Adam C. Martiny^{1,4}

- 1. Department of Earth System Science, University of California, Irvine, California 92697, USA
- 2. Department of Ecology and Evolutionary Biology, Princeton University, Princeton, New Jersey 08544, USA
- 3. Bigelow Laboratory for Ocean Sciences, East Boothbay, Maine 04544, USA
- 4. Department of Ecology and Evolutionary Biology, University of California, Irvine, California 92697, USA

Figures:

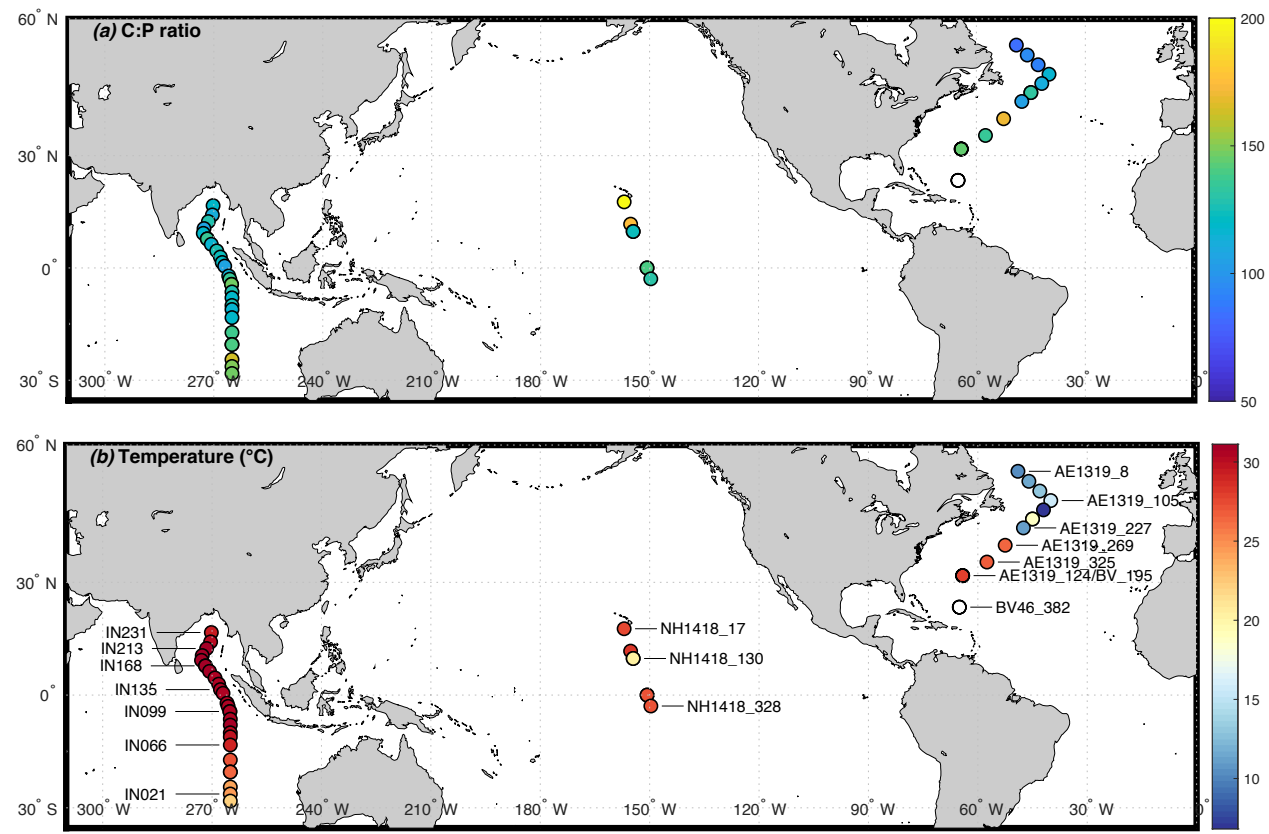
- 1. Cruise map.
- 2. Clade abundances
- 3. Total reads mapped.
- 4. Principle component analysis per nutrient genes.
- 5. Half saturation concentrations for phosphate.
- 6. Posterior for ATOM-gene Syn fit
- 7. Posterior for ATOM-gene Pro fit
- 8. Posterior predictive for ATOM-gene Syn fit
- 9. Posterior predictive for ATOM-gene Pro fit
- 10. Map of ATOM-gene traits

Tables:

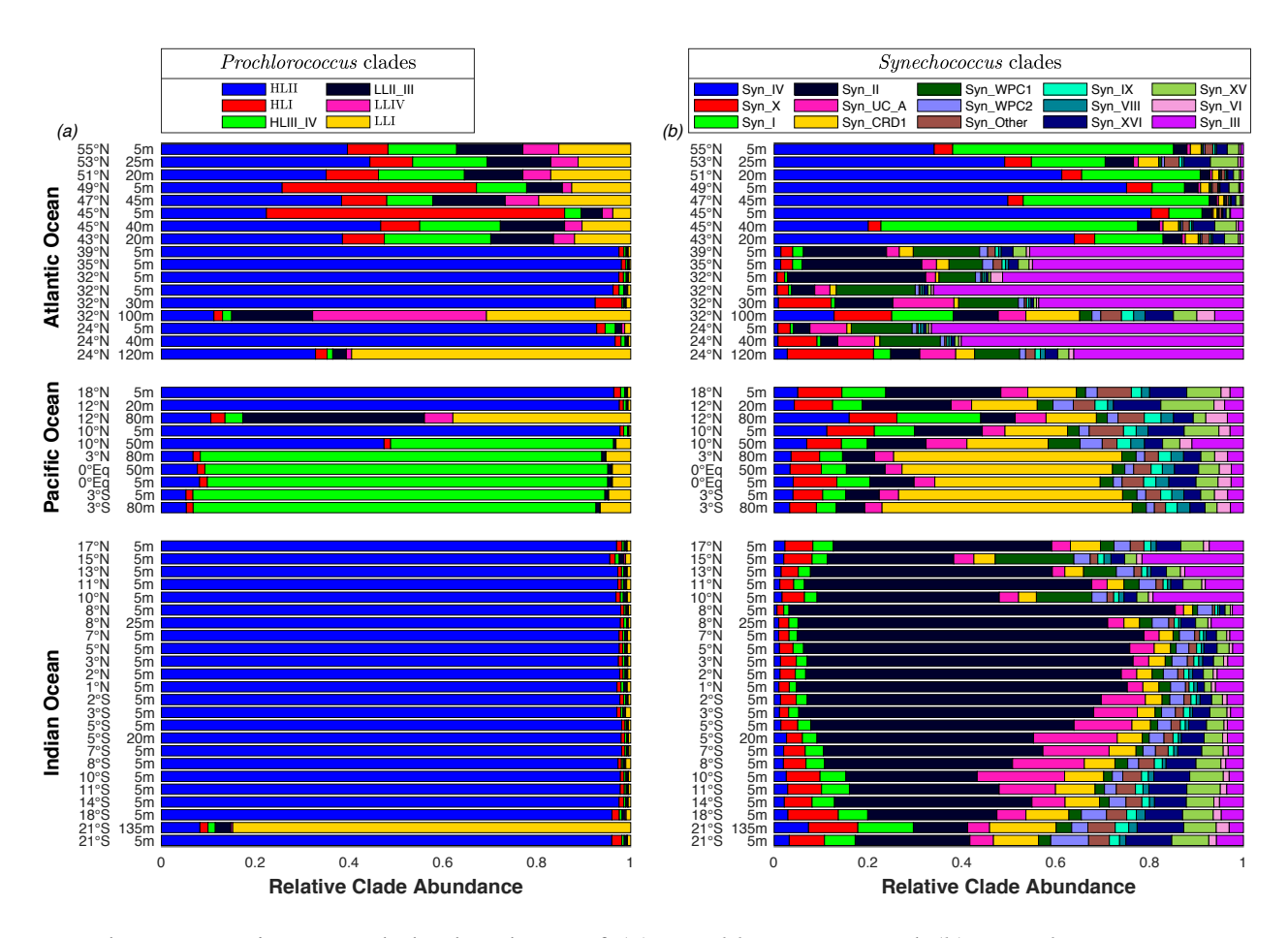
- 1. Particulate organic matter (C, N, P) and station information.
- 2. Inputs to ATOM-Gene and ATOM models.
- 3. Correlations for ATOM-Gene and *in situ* uptake kinetics
- 4. Genome and clade ids.
- 5. Fixed parameter definitions for ATOM
- 6. Statistical model parameter definitions for ATOM
- 7. Model comparisons
- 8. ATOM-gene Syn fit summary
- 9. ATOM-gene Pro fit summary

Additional data:

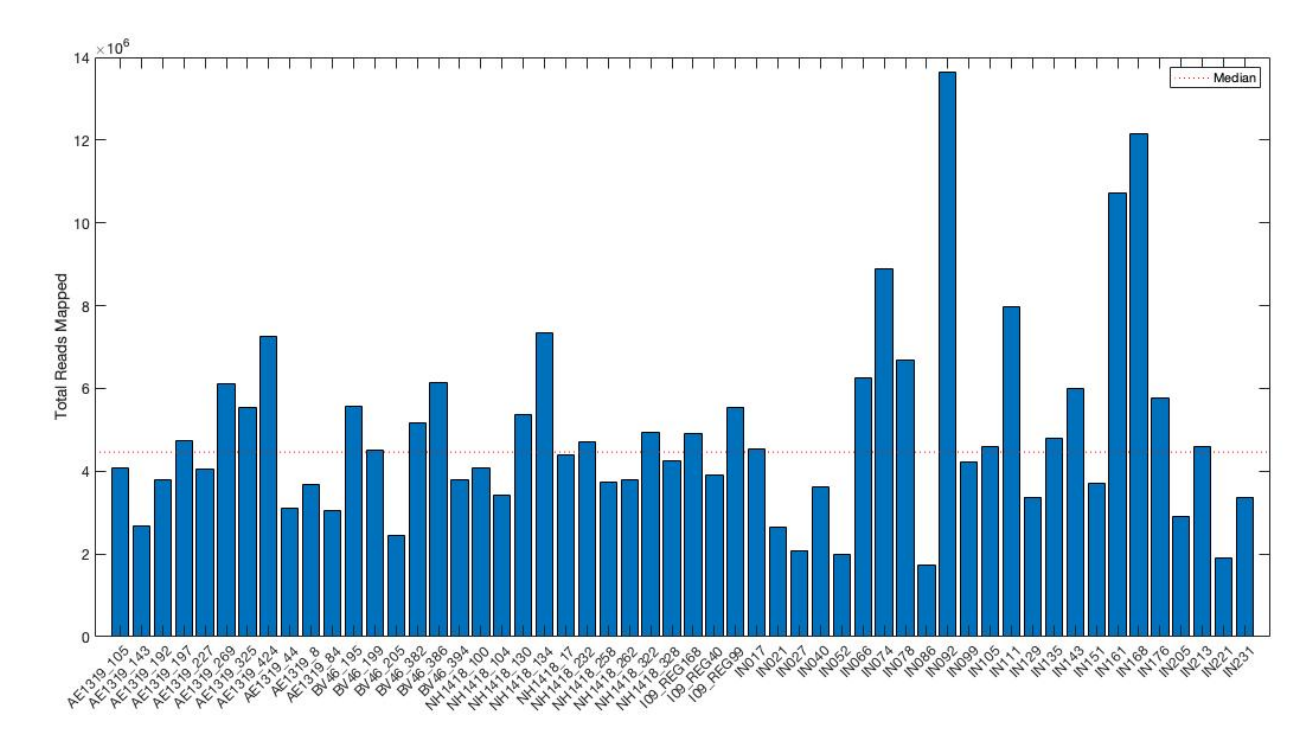
Supporting information 1: Table of nutrient assimilation genes



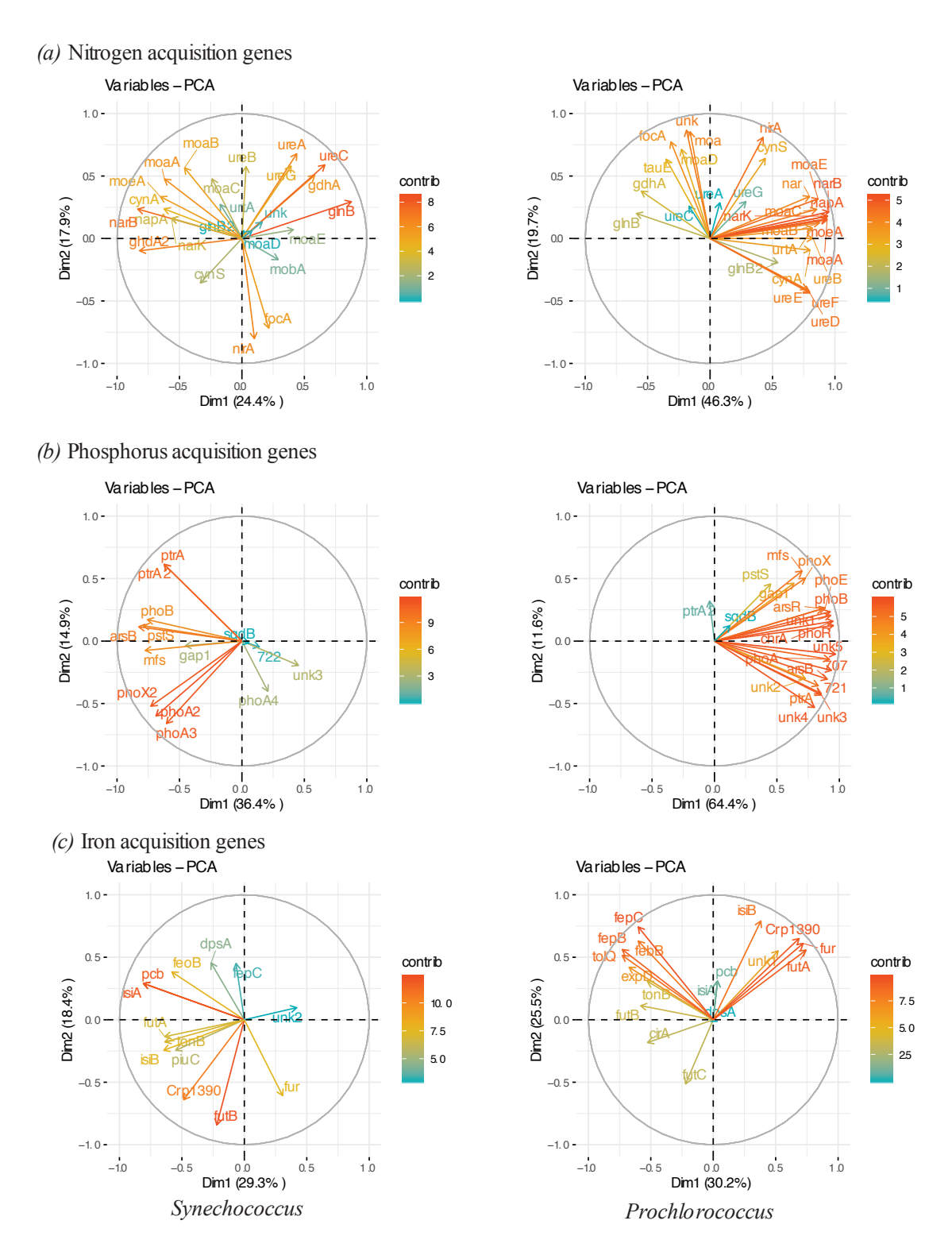
Supplementary Figure 1: Map of transects AE1319/BVAL46 (Atlantic), NH1418 (Pacific), and I09 (Indian Ocean). Observations for the a) C:P ratios and b) temperature (° Celsius) are shown with select stations labeled. Metagenomic samples AE1319_124 and BV46_195 are located at same site, but collected on different transects.



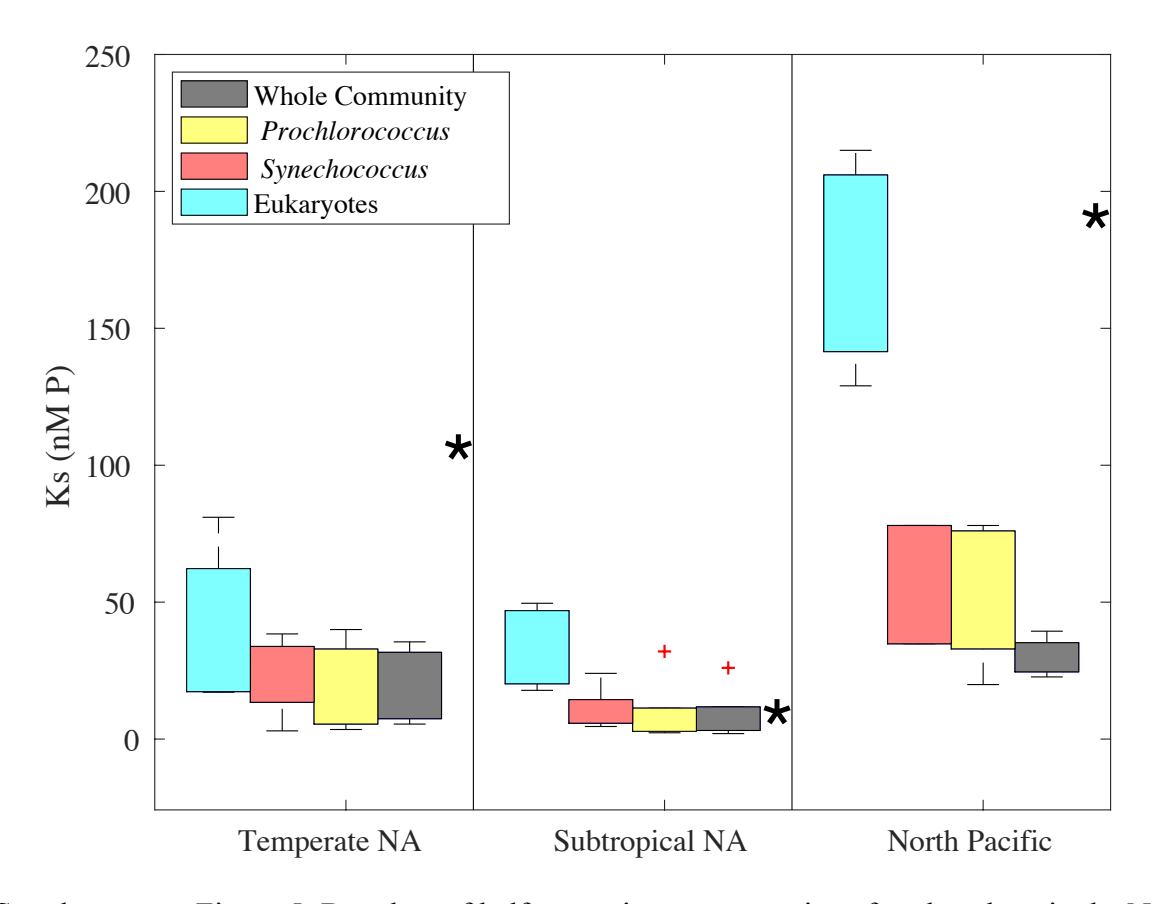
Supplementary Figure 2: Clade abundance of (a) Prochlorococcus and (b) Synechococcus according to supplementary table 4.



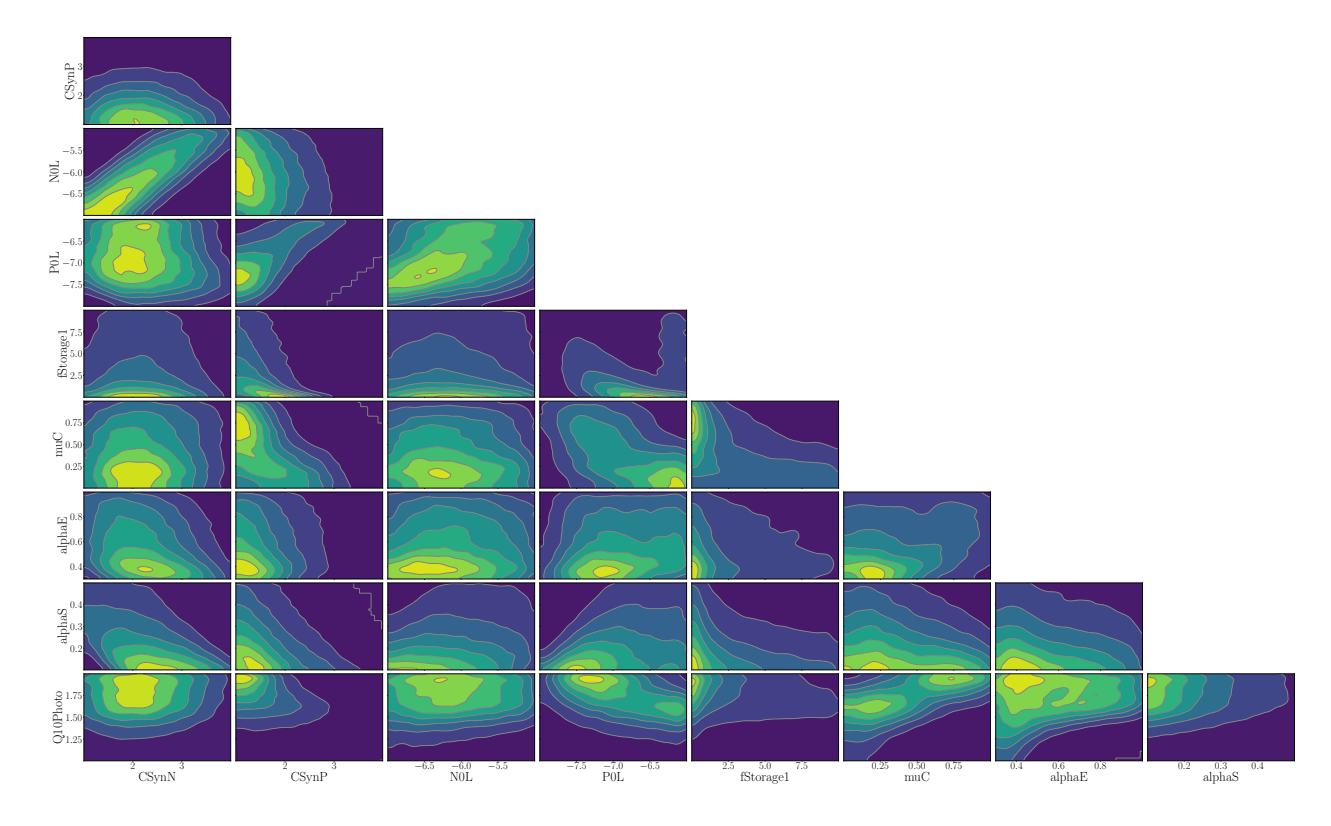
Supplementary Figure 3: Total reads mapped per station.



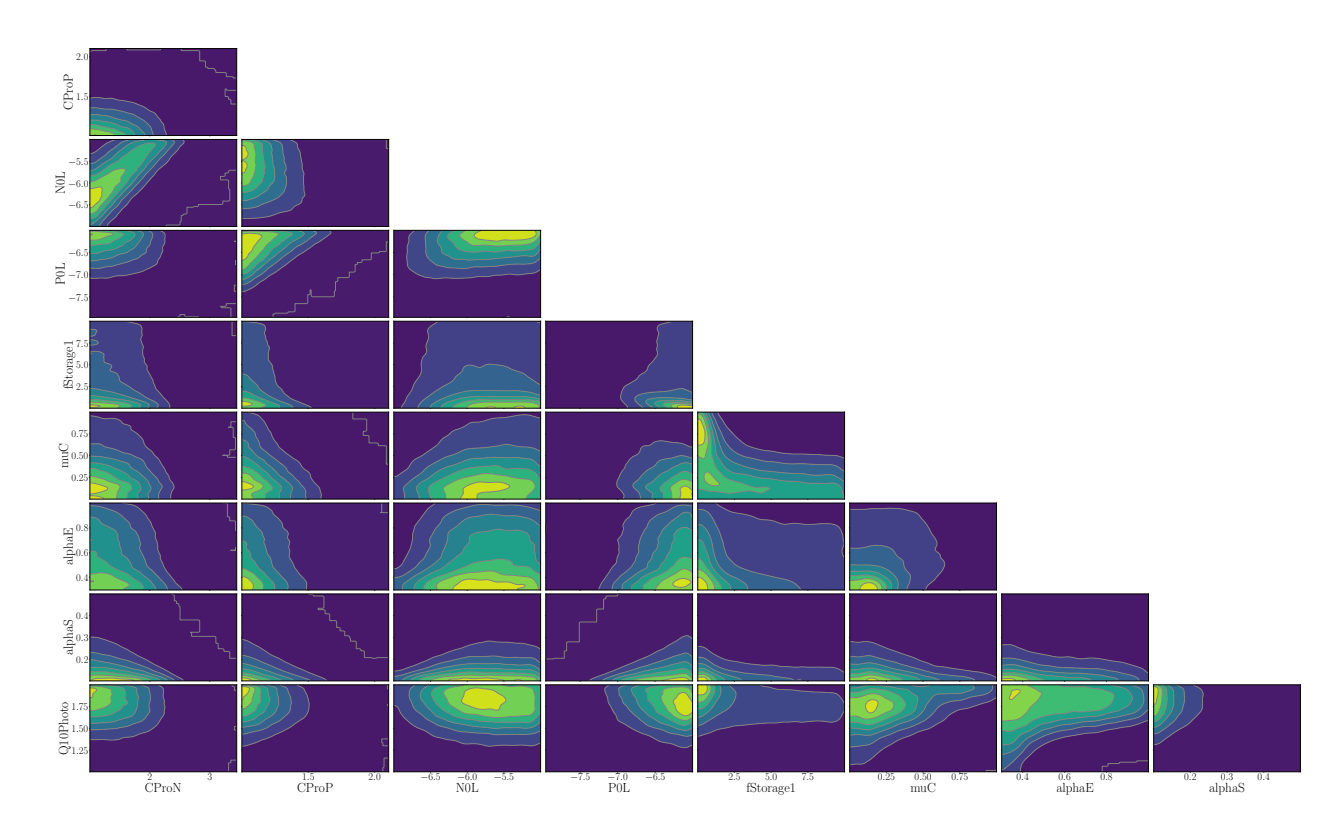
Supplementary Figure 4: Principle component analysis for stations using normalized gene coverages related to (a) Nitrogen, (b) Phosphorus, and (c) Iron acquisition.



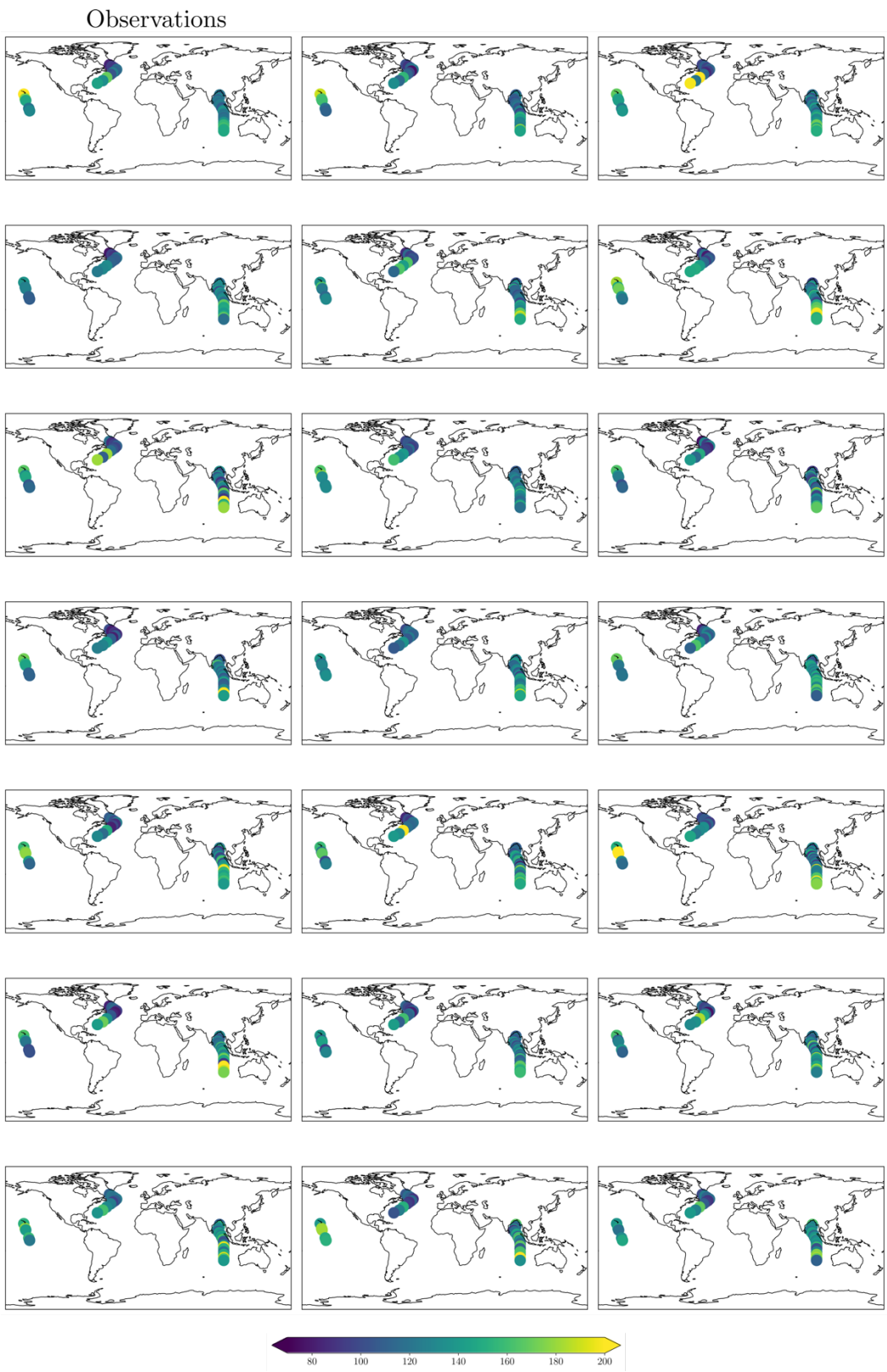
Supplementary Figure 5: Boxplots of half saturation concentrations for phosphate in the North Atlantic (NA) and Pacific oceans. Average ambient phosphate concentrations are shown with an asterisk (*) for each region.



Supplementary Figure 6: Pair-plot of posterior distribution for ATOM-gene model based on *Synechococcus* gene indices.

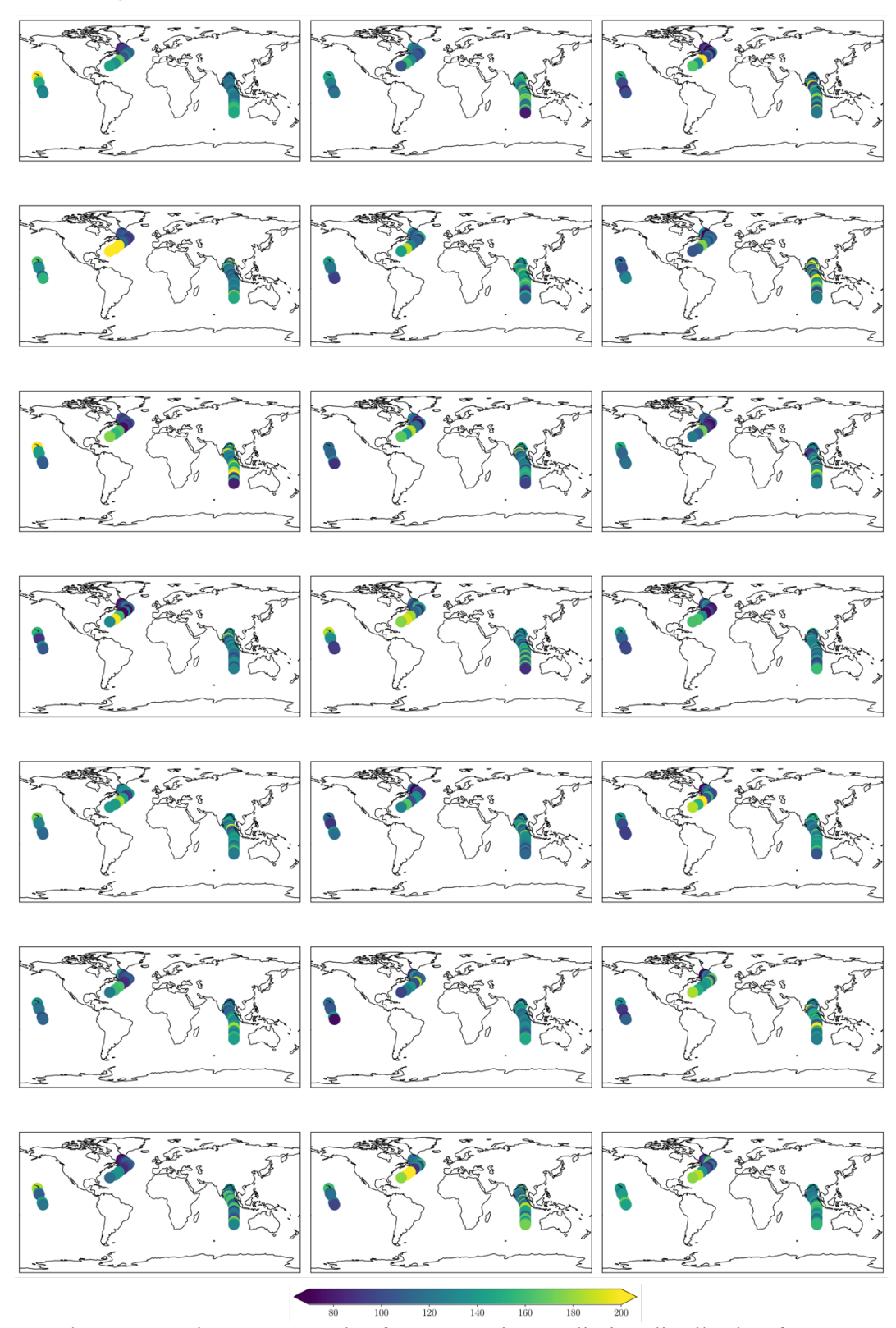


Supplementary Figure 7: Pair-plot of posterior distribution for ATOM-gene model based on *Prochlorococcus* gene indices.

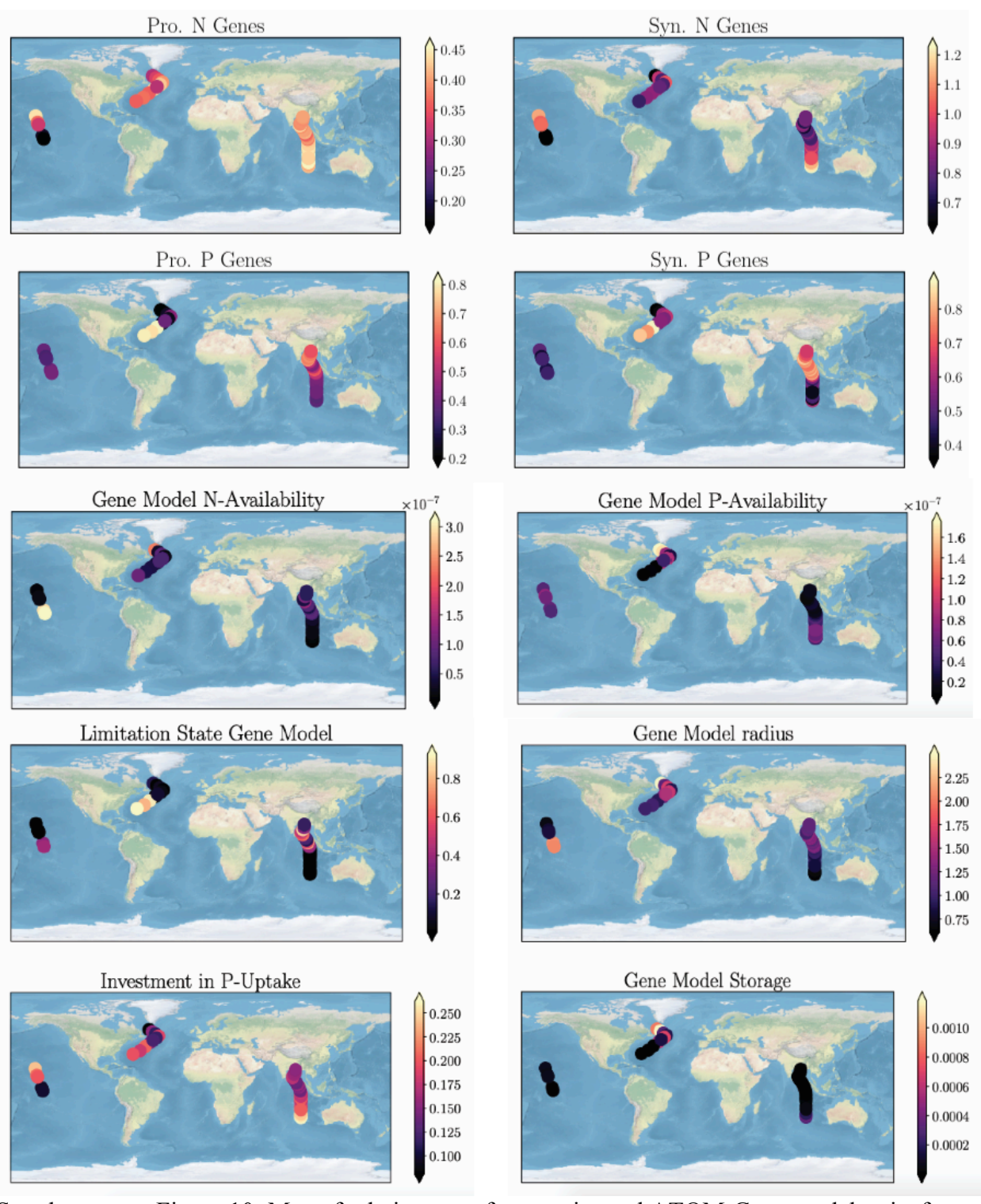


Supplementary Figure 8: Samples from posterior predictive distribution for ATOM-gene model based on *Synechococcus* gene indices.

Observations



Supplementary Figure 9: Samples from posterior predictive distribution for ATOM-gene model based on *Prochlorococcus* gene indices.



Supplementary Figure 10: Map of relative gene frequencies and ATOM-Gene model traits for *Synechococcus* (Syn) and *Prochlorococcus* (Pro).

Supplementary Table 1: Particulate organic matter observations for transects I09, NH1418, AE1319.

AL1317.				T		1				1
Metagenome										
SampleID	Latitude	Longitude	Depth	Datetime	POC	PON	POP	CN	CP	NP
unitless	[° N]	[°W]	[m]	unitless	[µmol/L]	[µmol/L]	[nmol/L]	unitless	unitless	unitless
AE1319_8	55.00	-49.00	5.00	26-Aug-2013	7.5	1.04	89.96	7.21	83.37	11.56
AE1319_44	53.00	-46.00	25.00	27-Aug-2013	11.52	1.52	121.62	7.58	94.72	12.50
AE1319 84	51.00	-43.00	20.00	28-Aug-2013	5.29	0.6	57.67	8.82	91.73	10.40
AE1319 105	49.00	-40.00	5.00	29-Aug-2013	5.66	0.63	48.06	8.98	117.77	13.11
AE1319 143	47.00	-42.00	45.00	30-Aug-2013	12.99	1.75	116.54	7.42	111.46	15.02
AE1319 197	45.00	-45.00	40.00	31-Aug-2013	14.51	1.91	120.7	7.60	120.22	15.82
AE1319 192	45.00	-45.00	5.00	31-Aug-2013	4.84	0.44	36.34	11.00	133.19	12.11
AE1319 227	43.00	-47.50	20.00	01-Sep-2013	7.16	0.98	68.43	7.31	104.63	14.32
AE1319 269	39.00	-52.50	5.00	03-Sep-2013	1.61	0.11	9.48	14.64	169.83	11.60
AE1319 325	35.00	-57.50	5.00	05-Sep-2013	1.58	0.17	11.67	9.29	135.39	14.57
AE1319_323 AE1319_424	31.67	-64.17	5.00		1.42	0.17	9.8	7.89	144.90	18.37
				08-Sep-2013						
BV46_195	31.67	-64.17	5.00	05-Oct-2011	nan	nan	9.58	nan	nan	nan
BV46_199	31.67	-64.17	30.00	05-Oct-2011	nan	nan	11.91	nan	nan	nan
BV46_205	31.67	-64.17	100.00	05-Oct-2011	nan	nan	5.49	nan	nan	nan
BV46_382	23.67	-65.07	5.00	11-Oct-2011	nan	nan	5.47	nan	nan	nan
BV46_386	23.67	-65.07	40.00	11-Oct-2011	nan	nan	6.72	nan	nan	nan
BV46_394	23.67	-65.07	120.00	11-Oct-2011	nan	nan	6.24	nan	nan	nan
NH1418_17	18.00	-157.00	5.00	20-Sep-2014	1.48	0.16	6	9.25	246.67	26.67
NH1418_104	12.00	-155.22	80.00	22-Sep-2014	1.5	0.21	13.26	7.14	113.12	15.84
NH1418_100	12.00	-155.22	20.00	22-Sep-2014	1.5	0.25	8.53	6.00	175.85	29.31
NH1418 130	10.00	-154.52	5.00	23-Sep-2014	1.71	0.25	9.92	6.84	172.38	25.20
NH1418 134	10.00	-154.52	50.00	23-Sep-2014	2.55	0.35	20.64	7.29	123.55	16.96
NH1418 232	3.00	-151.74	80.00	26-Sep-2014	1.99	0.32	17.65	6.22	112.75	18.13
NH1418 258	0.00	-150.70	50.00	27-Sep-2014	3.01	0.53	29.41	5.68	102.35	18.02
NH1418 262	0.00	-150.70	5.00	27-Sep-2014	3.96	0.69	28.35	5.74	139.68	24.34
NH1418 322	-3.00	-149.67	5.00	28-Sep-2014	2.63	0.42	20.06	6.26	131.11	20.94
NH1418 328	-3.00	-149.67	80.00	28-Sep-2014	2.34	0.39	20.75	6.00	112.77	18.80
IN231	17.00	89.80	5.00	24-Apr-2016	1.66	0.27	13.82	6.19	119.86	19.45
IN221	14.50	89.60	5.00	22-Apr-2016	1.65	0.27	14.64	6.70	112.58	16.82
IN213	12.70	88.50	5.00		1.03	0.25		6.57	128.96	19.65
				21-Apr-2016		0.20	13.25			
IN205	10.80	87.30	5.00	20-Apr-2016	1.90		17.57	6.62	107.99	16.31
IN176	9.50	87.10	5.00	16-Apr-2016	1.94	0.30	16.21	6.42	119.89	18.72
IN168	8.00	88.20	5.00	16-Apr-2016	2.08	0.33	18.35	6.29	113.25	18.14
I09_REG168	7.98	94.87	25.00	21-Mar-2016	2.06	0.31	15.33	6.73	134.44	19.91
IN161	6.50	89.30	5.00	15-Apr-2016	2.07	0.32	17.61	6.45	117.44	18.21
IN151	4.70	90.80	5.00	13-Apr-2016	1.93	0.30	15.31	6.37	125.80	19.90
IN143	3.00	91.80	5.00	12-Apr-2016	2.09	0.33	16.74	6.34	124.86	19.70
IN135	1.50	92.30	5.00	11-Apr-2016	1.81	0.31	14.86	5.86	122.09	20.87
IN129	0.50	93.00	5.00	11-Apr-2016	1.91	0.30	17.61	6.31	108.49	17.19
IN111	-2.20	94.10	5.00	08-Apr-2016	1.75	0.24	15.29	7.29	114.77	15.77
IN105	-3.10	94.40	5.00	08-Apr-2016	1.92	0.29	14.24	6.68	134.91	20.28
IN099	-4.50	94.90	5.00	07-Apr-2016	2.02	0.28	15.44	7.24	130.93	18.07
I09 REG99	-4.53	94.87	20.00	07-Apr-2016	1.88	0.27	12.75	7.00	147.80	21.26
IN092	-6.60	95.00	5.00	05-Apr-2016	1.70	0.27	13.31	6.32	127.69	20.22
IN086	-8.20	95.00	5.00	05-Apr-2016	1.59	0.24	13.24	6.60	119.89	18.16
IN078	-10.30	95.00	5.00	03-Apr-2016	1.85	0.30	14.71	6.32	125.99	20.13
IN074	-11.40	95.00	5.00	03-Apr-2016	1.78	0.31	15.29	5.84	116.29	19.95
IN066	-13.60	95.00	5.00	01-Apr-2016	1.54	0.26	12.85	6.04	119.96	19.91
IN052	-17.60	95.00	5.00	30-Mar-2016	1.63	0.20	11.76	7.33	138.35	18.92
I09 REG40	-20.76	95.00	20.00	29-Mar-2016	1.63	0.22	9.22	6.81	172.49	25.43
IN040	-20.80	95.00	5.00	29-Mar-2016	1.74	0.22	12.48	8.09	139.77	17.33
IN027	-24.70	95.00	5.00	26-Mar-2016	1.68	0.24	10.32	7.11	162.53	22.85
IN021	-26.50	95.00	5.00	25-Mar-2016	1.68	0.23	11.17	7.64	150.59	20.21
IN017	-28.30	95.00	5.00	25-Mar-2016	1.74	0.20	11.74	8.59	148.37	17.32

Supplementary Table 2: Inputs to ATOM models for transects I09, NH1418, AE1319. Temp = temperature, PAR = photosynthetically active radiation, PCA1 = first principle component in Sup. Fig. 4, P = phosphorus, N = nitrogen, Syn = Synechococcus, and Pro = Prochlorococcus.

Metagenome Station Temp. PAR PO4 P-gene N-Gene P-Gene N-Gene μmolPhotons/m2/s mol/I PCA1 Syn PCA1 Syn PCA1 Pro ID mol/I PCA1 Pro Celsius AE1319 8 4AE1319 10.38 118.27 1.70E-07 8.00E-07 -0.01 -0.85 -0.86 -1.66 AE1319 44 -1.43 5AE1319 11.73 124.44 1.70E-07 8.00E-07 -0.880.16 -0.67AE1319 84 6AE1319 13.23 131.75 7.00E-08 5.00E-09 -0.57 -0.30 -0.67 -1.40 AE1319 105 7AE1319 15.7 150.15 1.10E-07 5.00E-09 -0.51 -0.34 0.34 -0.98 AE1319 143 -1.21 8AE1319 6.82 158.45 1.50E-07 -0.29 5.00E-09 -0.64-0.63AE1319 192 9AE1319 13.53 174.31 1.10E-07 5.00E-09 -0.55 -0.15 0.22 -1.28 AE1319_227 10AE1319 11.19 138.66 1.60E-07 5.00E-09 -0.51 0.07 -0.71 -1.41 AE1319_269 154.08 0.08 12AE1319 26.29 5.00E-09 1.03 -0.60 2.13 5.00E-09 AE1319_325 0.28 14AE1319 26.58 146.34 5.00E-09 5.00E-09 0.82 -0.411.96 0.02 AE1319 424 16AE1319 27.93 170.15 5.00E-09 5.00E-09 0.94 -0.841.94 NH1418 17 2NH1418 27.7 213.95 0.82 -0.79 1.31 1.84E-07 1.00E-08 -0.26 NH1418 100 5NH1418 28.4 198.61 1.94E-07 1.00E-08 -0.35 0.71 -1.01 0.48 NH1418 130 7NH1418 24.45 157.19 -0.54 0.72 -0.31 2.62E-07 2.10E-07 -1.00NH1418 262 14NH1418 27.05 226.84 4.41E-07 4.41E-06 -0.46 0.31 -0.89 -1.41 NH1418 322 16NH1418 27.1 233.55 5.08E-07 5.74E-06 -0.62 0.13 -0.85 -1.55 IN231 194109 29.3896 237.12 5.00E-09 5.00E-09 0.06 0.17 0.44 0.62 IN221 189109 30.1723 241.27 5.00E-09 5.00E-09 0.59 -0.18 1.54 0.38 IN213 185I09 30.7808 244.49 5.00E-09 5.00E-09 0.37 -0.24 1.36 0.49 IN205 181109 31.1124 243.14 0.51 -0.33 1.24 0.36 5.00E-09 5.00E-09 237.93 0.87 IN176 166109 30.8228 5.00E-09 5.00E-09 0.50 -0.47 1.65 IN168 162109 31.1195 236.36 5.00E-09 5.00E-09 0.38 -0.53 0.13 0.53 IN161 158I09 30.8352 221.52 5.00E-08 0.21 -0.39 -0.41 0.61 5.00E-09 IN151 153109 30.5958 209.91 2.00E-08 5.00E-09 0.30 0.64 -0.35 -0.66 IN143 149109 30.5419 179.87 2.00E-08 5.00E-09 0.43 -0.51 0.09 0.60 IN135 145109 30.6921 176.72 1.00E-08 5.00E-09 0.36 -0.40 0.78 -0.13 IN129 142109 30.5922 196.79 1.00E-08 5.00E-09 0.60 -0.59 1.12 -0.09 IN111 133109 202.49 0.32 -0.37 0.03 0.47 30.6844 3.00E-08 5.00E-09 IN105 130109 30.7045 184.59 5.00E-09 5.00E-09 0.47 -0.28 -0.47 0.38 IN099 127109 30.4647 202.59 5.00E-09 5.00E-09 0.10 -0.19 -0.69 1.06 IN092 123I09 30.4743 181.97 3.00E-08 5.00E-09 -0.16 0.05 1.15 -0.68IN086 120109 30.7553 181.54 4.00E-08 5.00E-09 0.10 -0.17 -0.70 1.11 IN078 116I09 30.2587 171.33 6.00E-08 5.00E-09 -0.16 0.64 -0.75 1.24 IN074 114I09 29.7976 178.74 5.00E-08 5.00E-09 -0.140.76 -0.711.23 1.19 IN066 110I09 28.8714 160.28 5.00E-08 5.00E-09 -0.20 0.24 -0.79 IN052 103109 27.189 215.61 5.00E-08 5.00E-09 -0.50 0.50 -0.94 1.13 IN040 97109 26.2812 199.17 -0.42 0.85 0.59 8.00E-08 5.00E-09 -0.88 IN027 90109 24.1685 206.61 7.00E-08 5.00E-09 -0.42 0.98 -0.95 1.52 1.14 IN021 87109 24.2902 186.32 9.00E-08 5.00E-09 -0.540.86 -0.91 IN017 84109 22.3724 199.43 7.00E-08 5.00E-09 0.00 0.75 -0.98 1.04

Supplementary 3: Correlations between *in situ* observations, gene frequencies, and ATOM-Gene properties. Significant correlations (p-value < 0.05) are indicated by a star (*), with negative relationships in blue and positive in red.

R Correlation Coefficient	N gene freq Pro	P gene freq Pro	N gene freq Syn	P gene Freq Syn	NO3 rho	Urea rho	NH4 rho	CPObs
CP Literature T-regression model [mol C/mol P]	-0.55*	0.74*	-0.77*	0.79*	0.55*	0.67*	0.67*	-0.62*
CP Literature Trait model [mol C/mol P]	-0.53*	0.74*	-0.77*	0.75*	0.51*	0.64*	0.65*	-0.63*
CP P-regression model [mol C/mol P]	0.53*	-0.72*	0.79*	-0.79*	-0.56*	-0.68*	0.69*	0.64*
CP Pro Gene model [mol C/mol P]	0.78*	-0.48*	0.55*	-0.64*	-0.51*	-0.55*	0.44*	0.26
CP ATOM Syn Gene model [mol C/mol P]	0.44*	-0.47*	0.73	-0.61	-0.64	-0.66	-0.70	0.67*
CP T-regression model [mol C/mol P]	-0.37	0.54*	-0.87*	0.63*	0.67*	0.63*	0.81*	-0.80*
CP Literature T-regression mode [mol C/mol P]l	-0.38	0.54*	-0.87*	0.64*	0.67*	0.63*	0.81*	-0.80*
Biosynthesis investment Pro	-0.80*	0.51*	-0.59*	0.67*	0.54*	0.57*	0.47*	-0.29
Biosynthesis investment Syn	-0.44*	0.48*	-0.75*	0.62*	0.66*	0.67*	0.71*	-0.67*
Photosynthesis investment Pro	-0.83*	0.49*	-0.73*	0.73*	0.69*	0.60*	0.68*	-0.47*
Biosynthesis investment Syn	-0.44*	0.42*	-0.77*	0.61*	0.70*	0.62*	0.77*	-0.71*
N or P limitation Pro	-0.52*	0.86*	-0.37	0.49*	0.19	0.35	0.32	-0.46
N or P limitation Syn	-0.67*	0.68*	-0.77*	0.87*	0.75*	0.67*	0.75*	-0.58
N uptake affinity Pro								
[L/s]	-0.82*	0.43*	-0.69*	0.72*	0.69*	0.52*	0.65*	-0.34*
N uptake affinity Syn [L/s]	-0.34	0.25	-0.65*	0.46*	0.67*	0.55*	0.69*	-0.50*
N uptake rate Pro [mol N/s]	-0.68*	0.18	-0.44*	0.49*	0.46*	0.23	0.42*	-0.05
N uptake rate Syn [mol N/s]	-0.05	-0.09	-0.28	0.05	0.37	0.25	0.38	-0.21
P uptake affinity Pro [L/s]	-0.84*	0.45*	-0.69*	0.73*	0.69*	0.52*	0.65*	-0.35
P uptake affinity Syn [L/s]	-0.36	0.27	-0.66*	0.48*	0.68*	0.56*	0.70*	-0.51*
P uptake investment Pro	0.82*	-0.45*	0.66*	-0.69*	-0.63*	-0.57*	0.58*	0.35
P uptake investment Syn P quota (non-luxury) Pro	0.82*	-0.45*	0.66*	-0.69*	-0.63*	-0.57*	0.58*	0.35
[mol P/cell]	-0.71*	0.22	-0.48*	0.54*	0.51*	0.26	0.48*	-0.11
P quota (non-luxury) Syn [mol P/cell]	-0.07	-0.08	-0.30	0.08	0.40	0.27	0.40	-0.21
P uptake rate Pro [mol P/s]	-0.68*	0.18	-0.44*	0.49*	0.45*	0.23	0.42	-0.05
P uptake rate Syn [mol P/s]	-0.05	-0.09	-0.28	0.05	0.37	0.25	0.38	-0.21
Cell volume Pro [(mu m)^3]	-0.74*	0.27	-0.47*	0.54*	0.54*	0.26	0.51	-0.15
Cell volume Syn [(mu m)^3]	-0.13	-0.05	-0.36	0.14	0.47	0.32	0.46	-0.25
Cell radius Pro [mu m]	-0.81*	0.38	-0.61*	0.66*	0.62*	0.46*	0.57*	-0.25
Cell radius Syn [mu m]	-0.33	0.23	-0.62*	0.43*	0.65*	0.54*	0.66*	-0.48*

Supplementary Table 4: Genomes and clade assignments for *Prochlorococcus* and *Synechococcus*

Таха Genome Clade Synechococcus GEYO Syn.CRDI Synechococcus MITS9508 Syn.CRDI Synechococcus MITS9509 Syn.CRDI Synechococcus WH79A Syn.CRDI Synechococcus WH8016 Syn.I Synechococcus WH8016 Syn.I Synechococcus WH8020 Syn.I Synechococcus Syn.BI Syn.II Synechococcus N19 Syn.II Synechococcus Syn.BI Syn.II Synechococcus WH8102 Syn.II Synechococcus WH8109 Syn.II Synechococcus WH8109 Syn.II Synechococcus WH8102 Syn.II Synechococcus Syn.IV Syn.IV Synechococcus Syn.IV Synechococcus RS9916 Syn.IV Syn.IV Syn.Exhococcus Syn.IV Synechococcus KORDI 100 Syn.UC-A Synechococcus KORDI 52 Syn.WPC1 <t< th=""><th>synechoco</th><th>ccus</th><th></th></t<>	synechoco	ccus	
Synechococcus GEVO Syn.CRD1 Synechococcus MITS9508 Syn.CRD1 Synechococcus UW179A Syn.CRD1 Synechococcus CC9311 Syn.I Synechococcus WH8016 Syn.I Synechococcus WH8016 Syn.I Synechococcus WH8020 Syn.II Synechococcus N19 Syn.II Synechococcus N48102 Syn.II Synechococcus WH8109 Syn.II Synechococcus CC9902 Syn.II Synechococcus CC9902 Syn.IV Synechococcus NKBG042902 Syn.Other Synechococcus Sy9916 Syn.IX Synechococcus KORDI 100 Syn.UC-A Synechococcus KORDI 49 Syn.WI Synechococcus KORDI 52 Syn.	Taxa	Genome	Clade
Synechococcus MITS9508 Syn.CRD1 Synechococcus MITS9509 Syn.CRD1 Synechococcus CC9311 Syn.I Synechococcus UW179B Syn.I Synechococcus WH8016 Syn.I Synechococcus CC9605 Syn.II Synechococcus N19 Syn.II Synechococcus N19 Syn.II Synechococcus REDSEA S02 B4 Syn.II Synechococcus WH8109 Syn.II Synechococcus WH8109 Syn.II Synechococcus WH8102 Syn.III Synechococcus WH8102 Syn.IV Synechococcus RS9916 Syn.IV Synechococcus CC9616 Syn.IV Synechococcus KORDI 100 Syn.X Synechococcus KORDI 52 <			Svn CRD1
Synechococcus MITS9509 Syn.CRD1 Synechococcus UW179A Syn.CRD1 Synechococcus UW179B Syn.I Synechococcus WH8016 Syn.I Synechococcus WH8016 Syn.I Synechococcus WH8020 Syn.II Synechococcus N19 Syn.II Synechococcus N19 Syn.II Synechococcus N19 Syn.II Synechococcus N19 Syn.II Synechococcus WH8109 Syn.II Synechococcus WH8109 Syn.II Synechococcus WH8109 Syn.II Synechococcus WH8109 Syn.II Synechococcus CC9902 Syn.IV Synechococcus CC9902 Syn.IV Synechococcus RS9916 Syn.IV Synechococcus NKBG042902 Syn.Other Synechococcus KORDI 100 Syn.VI Synechococcus KORDI 100 Syn.VI Synechococcus KORDI 52 Sy			
Synechococcus UW179A Syn.CRD1 Synechococcus CC9311 Syn.I Synechococcus WH8016 Syn.I Synechococcus WH8016 Syn.I Synechococcus WH8020 Syn.II Synechococcus N19 Syn.II Synechococcus N19 Syn.II Synechococcus N4802 Syn.II Synechococcus N48109 Syn.II Synechococcus WH8109 Syn.II Synechococcus WH8102 Syn.IV Synechococcus CC9902 Syn.IV Synechococcus CC9902 Syn.IV Synechococcus RS9916 Syn.IX Synechococcus CC9616 Syn.UC-A Synechococcus PC7335 Syn.Other Synechococcus KORDI 100 Syn.UC-A Synechococcus KORDI 49 Syn.WPCI Synechococcus KORDI 52 Syn.WPCI Synechococcus KORDI 52 Syn.XY Synechococcus RCG007			
Synechococcus CC9311 Syn.1 Synechococcus UW179B Syn.1 Synechococcus WH8016 Syn.I Synechococcus WH8020 Syn.II Synechococcus CC9605 Syn.II Synechococcus N19 Syn.II Synechococcus REDSEA S02 B4 Syn.II Synechococcus WH8109 Syn.II Synechococcus WH8109 Syn.II Synechococcus WH8102 Syn.II Synechococcus WH8102 Syn.II Synechococcus CC9902 Syn.IV Synechococcus RS9916 Syn.IV Synechococcus RKBG042902 Syn.Other Synechococcus CC9616 Syn.UC-A Synechococcus KORDI 100 Syn.UC-A Synechococcus KORDI 100 Syn.UC-A Synechococcus KORDI 49 Syn.WPC2 Synechococcus KORDI 49 Syn.WPC2 Synechococcus GB101 Syn.X Synechococcus GB205<			
Synechococcus UW179B Syn.I Synechococcus WH8016 Syn.I Synechococcus WH8010 Syn.II Synechococcus CC9605 Syn.II Synechococcus N32 Syn.II Synechococcus N32 Syn.II Synechococcus UW86 Syn.II Synechococcus WH8109 Syn.II Synechococcus WH8109 Syn.II Synechococcus WH8102 Syn.III Synechococcus Syn.IV Syn.IV Synechococcus CC9902 Syn.IV Synechococcus NKBG042902 Syn.Other Synechococcus RS9916 Syn.IV Synechococcus KORDI Syn.UC-A Synechococcus KORDI Syn.UC-A Synechococcus KORDI Syn.VI Synechococcus KORDI Syn.WPCI Synechococcus KORDI Syn.XY Synechococcus GR0101 Syn.X Synechococcus GR01 Syn.XY			
Synechococcus WH8016 Syn.I Synechococcus WH8020 Syn.I Synechococcus N19 Syn.II Synechococcus N19 Syn.II Synechococcus N32 Syn.II Synechococcus WH8109 Syn.II Synechococcus WH8109 Syn.II Synechococcus WH8102 Syn.IV Synechococcus CC9902 Syn.IV Synechococcus RS9916 Syn.IV Synechococcus RS9916 Syn.IV Synechococcus RS9916 Syn.IV Synechococcus CC902 Syn.IV Synechococcus CC9016 Syn.IV Synechococcus CC9616 Syn.UC-A Synechococcus KORDI 100 Syn.UC-A Synechococcus KORDI 100 Syn.VI Synechococcus KORDI 49 Syn.VI Synechococcus KORDI 52 Syn.VII Synechococcus CB0101 Syn.X Synechococcus CB0205 Syn.X<			
Synechococcus WH8020 Syn.II Synechococcus CC9605 Syn.II Synechococcus N19 Syn.II Synechococcus REDSEA S02 B4 Syn.II Synechococcus REDSEA S02 B4 Syn.II Synechococcus WH8109 Syn.II Synechococcus WH8102 Syn.III Synechococcus BL107 Syn.IV Synechococcus RC9902 Syn.IV Synechococcus NKBG042902 Syn.Other Synechococcus NKBG042902 Syn.Other Synechococcus CC9616 Syn.UC-A Synechococcus KORDI 100 Syn.UC-A Synechococcus KORDI 100 Syn.UC-A Synechococcus KORDI 49 Syn.WPCI Synechococcus KORDI 52 Syn.WPCI Synechococcus KORDI 52 Syn.WPCI Synechococcus GFB01 Syn.X Synechococcus GR0101 Syn.X Synechococcus WH5701 Syn.X Synechococcus			
Synechococcus CC9605 Syn.II Synechococcus N19 Syn.II Synechococcus N32 Syn.II Synechococcus REDSEA S02 B4 Syn.II Synechococcus WH8109 Syn.II Synechococcus WH8109 Syn.III Synechococcus BL107 Syn.IV Synechococcus CC9902 Syn.IV Synechococcus CC9902 Syn.IV Synechococcus NKBG042902 Syn.Other Synechococcus PCC7335 Syn.Other Synechococcus KORDI 100 Syn.UC-A Synechococcus KORDI 100 Syn.UC-A Synechococcus KORDI 49 Syn.VIII Synechococcus KORDI 52 Syn.WPCI Synechococcus CB0101 Syn.X Synechococcus GE0205 Syn.X Synechococcus GE0205 Syn.X Synechococcus WH5701 Syn.X Synechococcus WH5701 Syn.XV Synechococcus WH5701			
Synechococcus N19 Syn.II Synechococcus N32 Syn.II Synechococcus NBSEA SO2 B4 Syn.II Synechococcus WH8109 Syn.II Synechococcus WH8102 Syn.III Synechococcus CS902 Syn.IV Synechococcus RS9916 Syn.IV Synechococcus NKBG042902 Syn.Other Synechococcus PCC7335 Syn.Other Synechococcus CC9616 Syn.UC-A Synechococcus KORDI 100 Syn.UC-A Synechococcus KORDI 100 Syn.WPC Synechococcus KORDI 49 Syn.WPC Synechococcus KORDI 49 Syn.WPC Synechococcus CB0101 Syn.X Synechococcus GB0101 Syn.X Synechococcus GB101 Syn.X Synechococcus GFB01 Syn.X Synechococcus WH5701 Syn.X Synechococcus WH5701 Syn.X Synechococcus WH5701			_
Synechococcus N32 Syn.II Synechococcus REDSEA SQ BYn.II Synechococcus WH8109 Syn.II Synechococcus WH8102 Syn.II Synechococcus WH8102 Syn.III Synechococcus BL107 Syn.IV Synechococcus CC9902 Syn.IV Synechococcus RS9916 Syn.IX Synechococcus NKBG042902 Syn.US Synechococcus NKBG042902 Syn.UY Synechococcus CC9616 Syn.UY Synechococcus KORDI 100 Syn.UC-A Synechococcus WH7805 Syn.VIII Synechococcus KORDI 49 Syn.WPC1 Synechococcus KORDI 52 Syn.WPC1 Synechococcus GB0101 Syn.X Synechococcus GE0101 Syn.X Synechococcus GFB01 Syn.X Synechococcus WH5701 Syn.X Synechococcus WH5701 Syn.XV Synechococcus <	Synechococcus		
Synechococcus REDSEA S02 B4 Syn.II Synechococcus UW86 Syn.II Synechococcus WH8109 Syn.III Synechococcus BL107 Syn.IV Synechococcus CC9902 Syn.IV Synechococcus NKBG042902 Syn.Other Synechococcus NKBG042902 Syn.Other Synechococcus KORDI 100 Syn.UC-A Synechococcus KORDI 100 Syn.UC-A Synechococcus KORDI 100 Syn.UC-A Synechococcus KORDI 49 Syn.VII Synechococcus KORDI 52 Syn.WPCI Synechococcus KORDI 52 Syn.WPCI Synechococcus GB010 Syn.X Synechococcus GB0205 Syn.X Synechococcus GRC307 Syn.X Synechococcus UW106 Syn.XV Synechococcus UW69 Syn.XV Synechococcus UW105 Syn.XVI Synechococcus UW106 Syn.XVI Synechococcus	Synechococcus	N19	Syn.II
Synechococcus UW86 Syn.II Synechococcus WH8109 Syn.II Synechococcus WH8102 Syn.IV Synechococcus CC9902 Syn.IV Synechococcus RS9916 Syn.IV Synechococcus RS9916 Syn.IX Synechococcus RS9916 Syn.IX Synechococcus PCC7335 Syn.Other Synechococcus CC9616 Syn.UC-A Synechococcus CC9616 Syn.UC-A Synechococcus RS9917 Syn.VI Synechococcus KORDI 100 Syn.UC-A Synechococcus KORDI 49 Syn.WPCI Synechococcus KORDI 52 Syn.WPCI Synechococcus CB0205 Syn.X Synechococcus GFB01 Syn.X Synechococcus WH5701 Syn.X Synechococcus WH5701 Syn.XV Synechococcus WH5701 Syn.XV Synechococcus UW69 Syn.XV Synechococcus WH5701	Synechococcus	N32	Syn.II
Synechococcus WH8109 Syn.II Synechococcus WH8102 Syn.III Synechococcus BL107 Syn.IV Synechococcus RS9916 Syn.IV Synechococcus RS9916 Syn.IV Synechococcus NKBG042902 Syn.Other Synechococcus CC9616 Syn.Uc-A Synechococcus KORDI 100 Syn.Uc-A Synechococcus KORDI 100 Syn.Uc-A Synechococcus KORDI 100 Syn.WPCI Synechococcus KORDI 49 Syn.WPCI Synechococcus KORDI 52 Syn.WPCI Synechococcus CB0101 Syn.X Synechococcus GB101 Syn.X Synechococcus GFB01 Syn.X Synechococcus WH5701 Syn.X Synechococcus UW106 Syn.XV Synechococcus UW69 Syn.XV Synechococcus UW105 Syn.XVI Synechococcus UW104 Syn.XVI Synechococcus EQPAC1 <td>Synechococcus</td> <td>REDSEA_S02_B4</td> <td>Syn.II</td>	Synechococcus	REDSEA_S02_B4	Syn.II
Synechococcus WH8109 Syn.II Synechococcus WH8102 Syn.III Synechococcus BL107 Syn.IV Synechococcus RS9916 Syn.IV Synechococcus RS9916 Syn.IV Synechococcus NKBG042902 Syn.Other Synechococcus CC9616 Syn.Uc-A Synechococcus KORDI 100 Syn.Uc-A Synechococcus KORDI 100 Syn.Uc-A Synechococcus KORDI 100 Syn.WPCI Synechococcus KORDI 49 Syn.WPCI Synechococcus KORDI 52 Syn.WPCI Synechococcus CB0101 Syn.X Synechococcus GB101 Syn.X Synechococcus GFB01 Syn.X Synechococcus WH5701 Syn.X Synechococcus UW106 Syn.XV Synechococcus UW69 Syn.XV Synechococcus UW105 Syn.XVI Synechococcus UW104 Syn.XVI Synechococcus EQPAC1 <td>Synechococcus</td> <td>UW86</td> <td>Syn.II</td>	Synechococcus	UW86	Syn.II
Synechococcus BL107 Syn.IV Synechococcus CC9902 Syn.IV Synechococcus NS9916 Syn.IX Synechococcus NKBG042902 Syn.Other Synechococcus PCC7335 Syn.Other Synechococcus KORDI 100 Syn.UC-A Synechococcus KORDI 100 Syn.UC-A Synechococcus KORDI 100 Syn.VII Synechococcus KORDI 49 Syn.VIII Synechococcus KORDI 52 Syn.VII Synechococcus CB0101 Syn.X Synechococcus CB0101 Syn.X Synechococcus CB0205 Syn.X Synechococcus GFB01 Syn.X Synechococcus WH5701 Syn.X Synechococcus UW106 Syn.XV Synechococcus UW69 Syn.XV Synechococcus UW105 Syn.XVI Synechococcus UW105 Syn.XVI Synechococcus UW106 Syn.XVI Synechococcus MED4	Synechococcus	WH8109	Syn.II
Synechococcus BL107 Syn.IV Synechococcus CC9902 Syn.IV Synechococcus NS9916 Syn.IX Synechococcus NKBG042902 Syn.Other Synechococcus PCC7335 Syn.Other Synechococcus KORDI 100 Syn.UC-A Synechococcus KORDI 100 Syn.UC-A Synechococcus KORDI 100 Syn.VII Synechococcus KORDI 49 Syn.VIII Synechococcus KORDI 52 Syn.VII Synechococcus CB0101 Syn.X Synechococcus CB0101 Syn.X Synechococcus CB0205 Syn.X Synechococcus GFB01 Syn.X Synechococcus WH5701 Syn.X Synechococcus UW106 Syn.XV Synechococcus UW69 Syn.XV Synechococcus UW105 Syn.XVI Synechococcus UW105 Syn.XVI Synechococcus UW106 Syn.XVI Synechococcus MED4	Synechococcus	WH8102	Svn.III
Synechococcus CC9902 Syn.IV Synechococcus RS9916 Syn.IV Synechococcus NRBG042902 Syn.Other Synechococcus CC9616 Syn.Uc-A Synechococcus KORDI 100 Syn.Uc-A Synechococcus KORDI 100 Syn.Uc-A Synechococcus RS9917 Syn.VII Synechococcus KORDI 49 Syn.WPCI Synechococcus KORDI 52 Syn.WPCI Synechococcus CB0101 Syn.X Synechococcus GB0205 Syn.X Synechococcus GB01 Syn.X Synechococcus WH5701 Syn.X Synechococcus WH06 Syn.XV Synechococcus UW106 Syn.XV Synechococcus UW108 Syn.XV Synechococcus UW109 Syn.XVI Synechococcus UW109 Syn.XVI Synechococcus UW109 Syn.XVI Synechococcus UW109 Syn.XVI Synechococcus UW109			
Synechococcus RS9916 Syn.IX Synechococcus NKBG042902 Syn.Other Synechococcus PCC7335 Syn.Other Synechococcus KORDI 100 Syn.UC-A Synechococcus WH7805 Syn.UC-A Synechococcus WH7805 Syn.VIII Synechococcus KORDI 49 Syn.WPC1 Synechococcus KORDI 52 Syn.WPC2 Synechococcus CB0101 Syn.X Synechococcus GB010 Syn.X Synechococcus GFB01 Syn.X Synechococcus GFB01 Syn.X Synechococcus WH5701 Syn.X Synechococcus UW106 Syn.XV Synechococcus UW105 Syn.XV Synechococcus UW105 Syn.XV Synechococcus UW105 Syn.XVI Synechococcus UW105 Syn.XVI Synechococcus UW105 Syn.XVI Synechococcus MED4 HL1 Prochlorococcus MED4			
Synechococcus NKBG042902 Syn.Other Synechococcus PCC7335 Syn.Other Synechococcus CC9616 Syn.UC-A Synechococcus WORDI 100 Syn.UC-A Synechococcus KORDI 100 Syn.VII Synechococcus RS9917 Syn.VII Synechococcus KORDI 49 Syn.WPC1 Synechococcus CB0101 Syn.X Synechococcus CB0101 Syn.X Synechococcus GFB01 Syn.X Synechococcus GFB01 Syn.X Synechococcus GFB01 Syn.X Synechococcus WH5701 Syn.X Synechococcus WH66 Syn.XV Synechococcus UW106 Syn.XV Synechococcus UW105 Syn.XV Synechococcus UW105 Syn.XVI Synechococcus UW105 Syn.XVI Synechococcus UW105 Syn.XVI Synechococcus UW106 Syn.XVI Syn.XVI Syn.XVI <td< td=""><td></td><td></td><td></td></td<>			
Synechococcus PCC7335 Syn.Other Synechococcus CC9616 Syn.UC-A Synechococcus KORDI 100 Syn.UC-A Synechococcus RS9917 Syn.VII Synechococcus RS9917 Syn.VII Synechococcus RS9917 Syn.VIII Synechococcus KORDI 49 Syn.WPCI Synechococcus CB0101 Syn.X Synechococcus CB0205 Syn.X Synechococcus GFB01 Syn.X Synechococcus WH5701 Syn.X Synechococcus WH5701 Syn.X Synechococcus UW106 Syn.XV Synechococcus UW69 Syn.XV Synechococcus UW105 Syn.XVI Synechococcus UW140 Syn.XVI Synechococcus UW140 Syn.XVI Synechococcus HED4 HLI Prochlorococcus MIT9515 HLI Prochlorococcus MIT9515 HLI Prochlorococcus MIT9123			
Synechococcus CC9616 Syn.UC-A Synechococcus KORDI 100 Syn.UC-A Synechococcus WH7805 Syn.UC-A Synechococcus KORDI 50 Syn.VIII Synechococcus KORDI 49 Syn.WPCI Synechococcus KORDI 52 Syn.WPCI Synechococcus CB0101 Syn.X Synechococcus GFB01 Syn.X Synechococcus GFB01 Syn.X Synechococcus WH5701 Syn.X Synechococcus UW106 Syn.XV Synechococcus UW106 Syn.XV Synechococcus UW105 Syn.XVI Synechococcus UW105 Syn.XVI Synechococcus UW105 Syn.XVI Synechococcus UW104 Syn.XVI Synechococcus UW104 Syn.XVI Synechococcus UW104 Syn.XVI Synechococcus HD9AC1 HLI Prochlorococcus MT9315 HLI Prochlorococcus AS9601 <			
Synechococcus KORDI 100 Syn.UC-A Synechococcus WH7805 Syn.VI Synechococcus RS9917 Syn.VII Synechococcus KORDI 49 Syn.WPCI Synechococcus KORDI 52 Syn.WPCI Synechococcus CB0101 Syn.X Synechococcus GFB01 Syn.X Synechococcus RCC307 Syn.X Synechococcus HK5701 Syn.X Synechococcus UW106 Syn.XV Synechococcus UW69 Syn.XV Synechococcus UW105 Syn.XVI Synechococcus UW105 Syn.XVI Synechococcus UW105 Syn.XVI Synechococcus HW104 Syn.XVI Synechococcus HW105 Syn.XVI Syn.XVI Syn.XVI Syn.XVI			
Synechococcus WH7805 Syn.VII Synechococcus RS9917 Syn.VII Synechococcus KORDI 49 Syn.WPCI Synechococcus CROIDI Syn.WPCI Synechococcus CB0101 Syn.X Synechococcus CB0205 Syn.X Synechococcus RCC307 Syn.X Synechococcus WH5701 Syn.X Synechococcus UW106 Syn.XV Synechococcus UW105 Syn.XV Synechococcus UW105 Syn.XVI Synechococcus UW105 Syn.XVI Synechococcus UW105 Syn.XVI Synechococcus UW105 Syn.XVI Synechococcus UW140 Syn.XVI Synechococcus UW140 Syn.XVI Synechococcus MED4 HLI Prochlorococcus MED4 HLI Prochlorococcus MIT9515 HLI Prochlorococcus MIT9201 HLII Prochlorococcus MIT9312 HLII			
Synechococcus RS9917 Syn.VIII Synechococcus KORDI 49 Syn.WPCI Synechococcus KORDI 52 Syn.WPCI Synechococcus CB0101 Syn.X Synechococcus CB0205 Syn.X Synechococcus GFB01 Syn.X Synechococcus WH5701 Syn.X Synechococcus WH5701 Syn.X Synechococcus UW106 Syn.XV Synechococcus UW108 Syn.XV Synechococcus UW109 Syn.XV Synechococcus UW109 Syn.XVI Synechococcus UW104 Syn.XVI Synechococcus EQPAC1 HL1 Prochlorococcus MED4 HL1 Prochlorococcus AS9601 HL1 Prochlorococcus MIT9515 HL1 Prochlorococcus MIT9201 HL1I Prochlorococcus MIT9213 HL1I Prochlorococcus MIT9301 HL1I Prochlorococcus MIT9312 HL1I <td></td> <td></td> <td></td>			
Synechococcus KORDI 49 Syn.WPC1 Synechococcus KORDI 52 Syn.WPC2 Synechococcus CB0101 Syn.X Synechococcus CB0205 Syn.X Synechococcus GFB01 Syn.X Synechococcus RCC307 Syn.X Synechococcus WH5701 Syn.X Synechococcus UW106 Syn.XV Synechococcus UW105 Syn.XV Synechococcus UW105 Syn.XV Synechococcus UW105 Syn.XVI Synechococcus EOPAC1 HL1 Prochlorococcus MED4 HL1 Prochlorococcus MED4 HL1 Prochlorococcus MT9515 HL1 Prochlorococcus MT9515 HL1 Prochlorococcus MT901 HL1I Prochlorococcus MT9123 HL1I Prochlorococcus MT9201 HL1I Prochlorococcus MT9312 HL1I Prochlorococcus MT9312 HL1I			
Synechococcus KORDI 52 Syn.WPC2 Synechococcus CB0101 Syn.X Synechococcus CB0205 Syn.X Synechococcus RCB0205 Syn.X Synechococcus RCC307 Syn.X Synechococcus WH5701 Syn.X Synechococcus UW106 Syn.XV Synechococcus UW105 Syn.XV Synechococcus UW105 Syn.XVI Synechococcus UW105 Syn.XVI Synechococcus EOPAC1 HLI Prochlorococcus MED4 HLI Prochlorococcus MED4 HLI Prochlorococcus MED4 HLI Prochlorococcus MED4 HLII Prochlorococcus MED4 HLII Prochlorococcus MIT9515 HLI Prochlorococcus MIT9201 HLII Prochlorococcus MIT923 HLII Prochlorococcus MIT9301 HLII Prochlorococcus MIT9314 HLII			
Synechococcus CB0101 Syn.X Synechococcus CB0205 Syn.X Synechococcus GFB01 Syn.X Synechococcus GFB01 Syn.X Synechococcus WH5701 Syn.X Synechococcus UW106 Syn.XV Synechococcus UW69 Syn.XV Synechococcus UW105 Syn.XVI Synechococcus UW106 Syn.XVI Synechococcus UW106 Syn.XVI Synechococcus UW106 Syn.XVI Synechococcus UW106 Syn.XVI Synechococcus EQPAC1 HL1 Prochlorococcus MED4 HL1 Prochlorococcus AS9601 HL1 Prochlorococcus MIT9123 HL11 Prochlorococcus MIT9201 HL11 Prochlorococcus MIT9301 HL11 Prochlorococcus MIT9301 HL11 Prochlorococcus MIT9312 HL11 Prochlorococcus MIT9314 HL11 <td></td> <td></td> <td></td>			
Synechococcus CB0205 Syn.X Synechococcus GFB01 Syn.X Synechococcus GFB01 Syn.X Synechococcus RCC307 Syn.X Synechococcus UW106 Syn.XV Synechococcus UW106 Syn.XV Synechococcus UW105 Syn.XVI Synechococcus UW105 Syn.XVI Synechococcus EQPAC1 HLI Prochlorococcus MED4 HLI Prochlorococcus MED4 HLI Prochlorococcus MT9515 HLI Prochlorococcus AS9601 HLII Prochlorococcus MT79604 HLII Prochlorococcus MT79123 HLII Prochlorococcus MT9215 HLII Prochlorococcus MT9301 HLII Prochlorococcus MT9312 HLII Prochlorococcus MT9312 HLII Prochlorococcus MT9312 HLII Prochlorococcus MT9401 HLII		_	Syn.WPC2
Synechococcus GFB01 Syn.X Synechococcus RCC307 Syn.X Synechococcus RCC307 Syn.X Synechococcus UW106 Syn.XV Synechococcus UW106 Syn.XV Synechococcus UW105 Syn.XVI Synechococcus UW140 Syn.XVI Synechococcus EQPACI HLI Prochlorococcus MED4 HLI Prochlorococcus MED4 HLI Prochlorococcus AS9601 HLII Prochlorococcus GP2 HLII Prochlorococcus MIT9604 HLII Prochlorococcus MIT9201 HLII Prochlorococcus MIT9215 HLII Prochlorococcus MIT9301 HLII Prochlorococcus MIT9312 HLII Prochlorococcus MIT9314 HLII Prochlorococcus MIT9312 HLII Prochlorococcus MIT9401 HLII Prochlorococcus SCGCAAA795 I06 HLII <td>Synechococcus</td> <td>CB0101</td> <td>Syn.X</td>	Synechococcus	CB0101	Syn.X
Synechococcus RCC307 Syn.X Synechococcus WH5701 Syn.X Synechococcus UW106 Syn.XV Synechococcus UW69 Syn.XV Synechococcus UW105 Syn.XVI Synechococcus UW105 Syn.XVI Synechococcus UW140 Syn.XVI Synechococcus EOPAC1 HLI Prochlorococcus MED4 HLI Prochlorococcus MED4 HLI Prochlorococcus ME9515 HLI Prochlorococcus AS9601 HLII Prochlorococcus MIT9123 HLII Prochlorococcus MIT9201 HLII Prochlorococcus MIT9301 HLII Prochlorococcus MIT9302 HLII Prochlorococcus MIT9312 HLII Prochlorococcus MIT9314 HLII Prochlorococcus MIT9312 HLII Prochlorococcus MIT9312 HLII Prochlorococcus SGGAAA795 106 HLII </td <td>Synechococcus</td> <td></td> <td>Syn.X</td>	Synechococcus		Syn.X
Synechococcus RCC307 Syn.X Synechococcus WH5701 Syn.X Synechococcus UW106 Syn.XV Synechococcus UW106 Syn.XV Synechococcus UW105 Syn.XVI Synechococcus UW105 Syn.XVI Synechococcus UW105 Syn.XVI Synechococcus UW140 Syn.XVI Prochlorococcus EOPAC1 HLI Prochlorococcus MED4 HLI Prochlorococcus MED4 HLI Prochlorococcus MS9601 HLII Prochlorococcus MIT91515 HLII Prochlorococcus MIT9204 HLII Prochlorococcus MIT9213 HLII Prochlorococcus MIT9312 HLII Prochlorococcus MIT9301 HLII Prochlorococcus MIT9312 HLII Prochlorococcus MIT9314 HLII Prochlorococcus MIT9314 HLII Prochlorococcus SCGCAAA795 106	Synechococcus	GFB01	Syn.X
Synechococcus WH5701 Syn.X Synechococcus UW106 Syn.XV Synechococcus UW69 Syn.XV Synechococcus UW105 Syn.XVI Synechococcus UW140 Syn.XVI Prochlorococcus EQPAC1 HL1 Prochlorococcus MED4 HL1 Prochlorococcus MED4 HL1 Prochlorococcus AS9601 HLII Prochlorococcus GP2 HLII Prochlorococcus MIT9123 HLII Prochlorococcus MIT9201 HLII Prochlorococcus MIT9201 HLII Prochlorococcus MIT9301 HLII Prochlorococcus MIT9312 HLII Prochlorococcus MIT9312 HLII Prochlorococcus MIT9314 HLII Prochlorococcus MIT9314 HLII Prochlorococcus MIT9401 HLII Prochlorococcus SG MIT9401 HLII Prochlorococcus SCGCAAA795 I06	Synechococcus	RCC307	Syn.X
Synechococcus UW106 Syn.XV Synechococcus UW69 Syn.XV Synechococcus UW105 Syn.XVI Synechococcus UW140 Syn.XVI Prochlorococcus EQPACI HLI Prochlorococcus MED4 HLI Prochlorococcus MED4 HLI Prochlorococcus MIT9515 HLI Prochlorococcus AS9601 HLII Prochlorococcus GP2 HLII Prochlorococcus MIT9123 HLII Prochlorococcus MIT9201 HLII Prochlorococcus MIT9301 HLII Prochlorococcus MIT9312 HLII Prochlorococcus MIT9312 HLII Prochlorococcus MIT9312 HLII Prochlorococcus MIT9314 HLII Prochlorococcus MIT9312 HLII Prochlorococcus MIT9401 HLII Prochlorococcus SCGCAAA795 106 HLII Prochlorococcus SCGCAAA795 M23		WH5701	Syn.X
Synechococcus UW69 Syn.XV Synechococcus UW105 Syn.XVI Synechococcus UW140 Syn.XVI Synechococcus UW140 Syn.XVI Prochlorococcus MED4 HLI Prochlorococcus MED4 HLI Prochlorococcus MED4 HLI Prochlorococcus MIT9515 HLI Prochlorococcus MIT0604 HLII Prochlorococcus MIT923 HLII Prochlorococcus MIT9201 HLII Prochlorococcus MIT9301 HLII Prochlorococcus MIT9302 HLII Prochlorococcus MIT9302 HLII Prochlorococcus MIT9314 HLII Prochlorococcus MIT9322 HLII Prochlorococcus SB HLII Prochlorococcus SB HLII Prochlorococcus SCGCAAA795 106 HLII Prochlorococcus SCGCAAA795 M23 HLII Prochlorococcus HNLC1 HLI			
Synechococcus UW105 Syn.XVI Synechococcus UW140 Syn.XVI Prochlorococcus EQPAC1 HLI Prochlorococcus EQPAC1 HLI Prochlorococcus MED4 HLI Prochlorococcus MIT9515 HLI Prochlorococcus AS9601 HLII Prochlorococcus MIT0604 HLII Prochlorococcus MIT9123 HLII Prochlorococcus MIT9201 HLII Prochlorococcus MIT9301 HLII Prochlorococcus MIT9302 HLII Prochlorococcus MIT9312 HLII Prochlorococcus MIT9314 HLII Prochlorococcus MIT9314 HLII Prochlorococcus MIT9401 HLII Prochlorococcus SB HLII Prochlorococcus SGGCAAA795 I06 HLII Prochlorococcus SCGCAAA795 I15 HLII Prochlorococcus SCGCAAA795 M23 HLII Prochlorococcus HNILC1			
Synechococcus UW140 Syn.XVI Prochlorococcus EQPACI HLI Prochlorococcus MEDA HLI Prochlorococcus MEDA HLI Prochlorococcus AS9601 HLII Prochlorococcus GP2 HLII Prochlorococcus MIT0604 HLII Prochlorococcus MIT9213 HLII Prochlorococcus MIT9215 HLII Prochlorococcus MIT9301 HLII Prochlorococcus MIT9302 HLII Prochlorococcus MIT9312 HLII Prochlorococcus MIT9314 HLII Prochlorococcus MIT9312 HLII Prochlorococcus MIT9401 HLII Prochlorococcus SCGCAAA795 MIT Prochlorococcus SCGCAAA795 MIT Prochlorococcus SCGCAAA795 MIT Prochlorococcus HNLC1 HLIII-IV Prochlorococcus HNLC2 HLIII-IV Prochlorococcus XMU1403			
Prochlorococcus EQPAC1 HLI Prochlorococcus MED4 HLI Prochlorococcus MED4 HLI Prochlorococcus MIT9515 HLI Prochlorococcus MIT9515 HLI Prochlorococcus GP2 HLII Prochlorococcus MIT9604 HLII Prochlorococcus MIT9201 HLII Prochlorococcus MIT9201 HLII Prochlorococcus MIT9301 HLII Prochlorococcus MIT9302 HLII Prochlorococcus MIT9312 HLII Prochlorococcus MIT9314 HLII Prochlorococcus MIT9322 HLII Prochlorococcus SCGCAAA795 HLII Prochlorococcus SCGCAAA795 HLII Prochlorococcus SCGCAAA795 HLII Prochlorococcus SCGCAAA795 HLII Prochlorococcus HNLC1 HLIII-IV Prochlorococcus RS50 HLII Prochlorococcus MU1401			
Prochlorococcus MED4 HLI Prochlorococcus MIT9515 HLI Prochlorococcus GP2 HLII Prochlorococcus GP2 HLII Prochlorococcus MIT0604 HLII Prochlorococcus MIT9123 HLII Prochlorococcus MIT9201 HLII Prochlorococcus MIT9301 HLII Prochlorococcus MIT9302 HLII Prochlorococcus MIT9312 HLII Prochlorococcus MIT9314 HLII Prochlorococcus MIT9322 HLII Prochlorococcus SMT9314 HLII Prochlorococcus SEGCAAA795 II6 HLII Prochlorococcus SCGCAAA795 II6 HLII Prochlorococcus SCGCAAA795 II6 HLII Prochlorococcus SCGCAAA795 II15 HLII Prochlorococcus HNLC1 HLIII-IV Prochlorococcus RS50 HLII Prochlorococcus XMU1403 LLI Prochlorococcus			
Prochlorococcus MIT9515 HLI Prochlorococcus AS9601 HLII Prochlorococcus AS9601 HLII Prochlorococcus MIT0604 HLII Prochlorococcus MIT9123 HLII Prochlorococcus MIT9201 HLII Prochlorococcus MIT9215 HLII Prochlorococcus MIT9301 HLII Prochlorococcus MIT9312 HLII Prochlorococcus MIT9314 HLII Prochlorococcus MIT9314 HLII Prochlorococcus MIT9312 HLII Prochlorococcus MIT9401 HLII Prochlorococcus SB HLII Prochlorococcus SCGCAAA795 II Prochlorococcus SCGCAAA795 II Prochlorococcus HNILC1 HLIII-IV Prochlorococcus HNILC2 HLIII-IV Prochlorococcus XMU1403 HLI Prochlorococcus NATL1A LLI Prochlorococcus NATL2A	Dun al-lana an anna		
Prochlorococcus AS9601 HLII Prochlorococcus GP2 HLII Prochlorococcus MIT0604 HLII Prochlorococcus MIT0201 HLII Prochlorococcus MIT9201 HLII Prochlorococcus MIT9301 HLII Prochlorococcus MIT9302 HLII Prochlorococcus MIT9312 HLII Prochlorococcus MIT9312 HLII Prochlorococcus MIT9314 HLII Prochlorococcus MIT9322 HLII Prochlorococcus SB HLII Prochlorococcus SCGCAAA795 I06 HLII Prochlorococcus SCGCAAA795 I15 HLII Prochlorococcus SCGCAAA795 IN3 HLII Prochlorococcus HNLC1 HLIII-IV Prochlorococcus HNLC2 HLIII-IV Prochlorococcus XMU1401 HLII Prochlorococcus XMU1403 LLI Prochlorococcus NATL1A LLI Prochlorococcus <t< td=""><td></td><td></td><td></td></t<>			
Prochlorococcus GP2 HLII Prochlorococcus MIT0604 HLII Prochlorococcus MIT9123 HLII Prochlorococcus MIT9201 HLII Prochlorococcus MIT9201 HLII Prochlorococcus MIT9301 HLII Prochlorococcus MIT9302 HLII Prochlorococcus MIT9312 HLII Prochlorococcus MIT9314 HLII Prochlorococcus MIT9322 HLII Prochlorococcus SB HLII Prochlorococcus SCGCAAA795 I06 HLII Prochlorococcus SCGCAAA795 I15 HLII Prochlorococcus SCGCAAA795 M23 HLII Prochlorococcus HNLC1 HLIII-IV Prochlorococcus RS50 HLII Prochlorococcus XMU1401 HLII Prochlorococcus XMU1403 LLI Prochlorococcus NATL1A LLI Prochlorococcus NATL2A LLI Prochlorococcus MIT			
Prochlorococcus MIТ0604 HLII Prochlorococcus MIТ9123 HLII Prochlorococcus MIT9201 HLII Prochlorococcus MIT9215 HLII Prochlorococcus MIT9301 HLII Prochlorococcus MIT9302 HLII Prochlorococcus MIT9314 HLII Prochlorococcus MIT9312 HLII Prochlorococcus MIT9312 HLII Prochlorococcus MIT9314 HLII Prochlorococcus MIT9401 HLII Prochlorococcus SB HLII Prochlorococcus SCGCAAA795 I06 HLII Prochlorococcus SCGCAAA795 I15 HLII Prochlorococcus SCGCAAA795 I15 HLII Prochlorococcus HNLC1 HLIII-IV Prochlorococcus HNLC2 HLIII-IV Prochlorococcus XMU1401 HLII Prochlorococcus XMU1403 LLI Prochlorococcus NATL1A LLI Prochlorococcus			
Prochlorococcus MIT9123 HLII Prochlorococcus MIT9201 HLII Prochlorococcus MIT9301 HLII Prochlorococcus MIT9301 HLII Prochlorococcus MIT9302 HLII Prochlorococcus MIT9312 HLII Prochlorococcus MIT9314 HLII Prochlorococcus MIT9322 HLII Prochlorococcus MIT9401 HLII Prochlorococcus SCGCAAA795 II Prochlorococcus SCGCAAA795 II Prochlorococcus SCGCAAA795 MIT Prochlorococcus HNLC1 HLII Prochlorococcus HNLC2 HLIII-IV Prochlorococcus XMU1403 LLI Prochlorococcus XMU1403 LLI Prochlorococcus NATL1A LLI Prochlorococcus NATL1A LLI Prochlorococcus NATL1A LLI Prochlorococcus MIT0601 LLII-III Prochlorococcus MIT0601 </td <td></td> <td></td> <td></td>			
Prochlorococcus MIT9201 HLII Prochlorococcus MIT9215 HLII Prochlorococcus MIT9301 HLII Prochlorococcus MIT9302 HLII Prochlorococcus MIT9312 HLII Prochlorococcus MIT9314 HLII Prochlorococcus MIT9314 HLII Prochlorococcus MIT9322 HLII Prochlorococcus SCGCAAA795 HLII Prochlorococcus SCGCAAA795 HLII Prochlorococcus SCGCAAA795 II5 Prochlorococcus SCGCAAA795 MLII Prochlorococcus HNLC1 HLIII-IV Prochlorococcus HNLC2 HLIII-IV Prochlorococcus XMU1401 HLII Prochlorococcus XMU1403 LLI Prochlorococcus NATL1A LLI Prochlorococcus NATL1A LLI Prochlorococcus NATL1A LLI Prochlorococcus MIT0601 LLII-III Prochlorococcus <t< td=""><td></td><td></td><td></td></t<>			
Prochlorococcus MIT9215 HLII Prochlorococcus MIT9301 HLII Prochlorococcus MIT9302 HLII Prochlorococcus MIT9312 HLII Prochlorococcus MIT9314 HLII Prochlorococcus MIT9322 HLII Prochlorococcus SIT9322 HLII Prochlorococcus SB HLII Prochlorococcus SCGCAAA795 II6 Prochlorococcus SCGCAAA795 II5 Prochlorococcus SCGCAAA795 MLII Prochlorococcus HNLC1 HLIII-IV Prochlorococcus HNLC2 HLIII-IV Prochlorococcus XMU1401 HLII Prochlorococcus XMU1403 LLI Prochlorococcus NATUA LLI Prochlorococcus NATLA LLI Prochlorococcus NATLA LLI Prochlorococcus MIT0801 LLI Prochlorococcus MIT0601 LLII-III Prochlorococcus MIT0601 <td></td> <td></td> <td></td>			
Prochlorococcus MIT9301 HLII Prochlorococcus MIT9302 HLII Prochlorococcus MIT9312 HLII Prochlorococcus MIT9314 HLII Prochlorococcus MIT9322 HLII Prochlorococcus MIT9322 HLII Prochlorococcus SB HLII Prochlorococcus SEGCAAA795 II6 Prochlorococcus SCGCAAA795 II5 Prochlorococcus SCGCAAA795 M23 Prochlorococcus HNLC1 HLII Prochlorococcus HNLC2 HLIII-IV Prochlorococcus RSS0 HLII Prochlorococcus XMU1403 LLI Prochlorococcus XMU1408 LLI Prochlorococcus NATL1A LLI Prochlorococcus NATL2A LLI Prochlorococcus MIT0801 LLII-III Prochlorococcus MIT0601 LLII-III Prochlorococcus MIT0601 LLII-III Prochlorococcus MIT060	Prochlorococcus		
Prochlorococcus MIT9302 HLII Prochlorococcus MIT9312 HLII Prochlorococcus MIT9314 HLII Prochlorococcus MIT9322 HLII Prochlorococcus MIT9401 HLII Prochlorococcus SB HLII Prochlorococcus SCGCAAA795 106 HLII Prochlorococcus SCGCAAA795 115 HLII Prochlorococcus SCGCAAA795 M23 HLII Prochlorococcus HNLC1 HLIII-IV Prochlorococcus HNLC2 HLIII-IV Prochlorococcus RS50 HLII Prochlorococcus XMU1403 LLI Prochlorococcus XMU1408 LLI Prochlorococcus NATL1A LLI Prochlorococcus NATL2A LLI Prochlorococcus MIT0801 LLII-III Prochlorococcus MIT0601 LLII-III Prochlorococcus MIT0601 LLII-III Prochlorococcus MIT0701 LLII-III Prochlorococcus			
Prochlorococcus MIT9312 HLII Prochlorococcus MIT9314 HLII Prochlorococcus MIT9312 HLII Prochlorococcus MIT9401 HLII Prochlorococcus SB HLII Prochlorococcus SCGCAAA795 I06 HLII Prochlorococcus SCGCAAA795 II5 HLII Prochlorococcus SCGCAAA795 M23 HLII Prochlorococcus HNLC1 HLIII-IV Prochlorococcus HNLC2 HLIII-IV Prochlorococcus KMU1401 HLII Prochlorococcus XMU1403 LLI Prochlorococcus XMU1408 LLI Prochlorococcus NATL1A LLI Prochlorococcus NATL2A LLI Prochlorococcus MATL2A LLI Prochlorococcus MIT0601 LLII-III Prochlorococcus MIT0602 LLII-III Prochlorococcus MIT0701 LLIV-III Prochlorococcus MIT1312 LLIV Prochlorococcus <td>Prochlorococcus</td> <td></td> <td>HLII</td>	Prochlorococcus		HLII
Prochlorococcus MIT9314 HLII Prochlorococcus MIT9322 HLII Prochlorococcus MIT9401 HLII Prochlorococcus SB HLII Prochlorococcus SCGCAAA795 I06 HLII Prochlorococcus SCGCAAA795 I15 HLII Prochlorococcus SCGCAAA795 M23 HLII Prochlorococcus HNLC1 HLIII-IV Prochlorococcus HNLC2 HLIII-IV Prochlorococcus XMU1401 HLII Prochlorococcus XMU1403 LLI Prochlorococcus XMU1408 LLI Prochlorococcus NATL1A LLI Prochlorococcus NATL1A LLI Prochlorococcus MATL2A LLI Prochlorococcus MIT0601 LLII-III Prochlorococcus MIT0601 LLII-III Prochlorococcus MIT0601 LLII-III Prochlorococcus MIT0701 LLIV-III Prochlorococcus MIT1312 LLIV Prochlorococcus	Prochlorococcus	MIT9302	HLII
Prochlorococcus MIT9314 HLII Prochlorococcus MIT9322 HLII Prochlorococcus MIT9401 HLII Prochlorococcus SB HLII Prochlorococcus SCGCAAA795 I06 HLII Prochlorococcus SCGCAAA795 I15 HLII Prochlorococcus SCGCAAA795 M23 HLII Prochlorococcus HNLC1 HLIII-IV Prochlorococcus HNLC2 HLIII-IV Prochlorococcus XMU1401 HLII Prochlorococcus XMU1403 LLI Prochlorococcus XMU1408 LLI Prochlorococcus NATL1A LLI Prochlorococcus NATL1A LLI Prochlorococcus MATL2A LLI Prochlorococcus MIT0601 LLII-III Prochlorococcus MIT0601 LLII-III Prochlorococcus MIT0601 LLII-III Prochlorococcus MIT0701 LLIV-III Prochlorococcus MIT1312 LLIV Prochlorococcus	Prochlorococcus	MIT9312	HLII
Prochlorococcus MIT9322 H.LII Prochlorococcus MIT9401 H.LII Prochlorococcus MIT9401 H.LII Prochlorococcus SCB H.LII Prochlorococcus SCGCAAA795 106 H.LII Prochlorococcus SCGCAAA795 115 H.LII Prochlorococcus SCGCAAA795 M23 H.LII Prochlorococcus HNLC1 H.LIII-IV Prochlorococcus HNLC2 H.LIII-IV Prochlorococcus XSS0 H.LII Prochlorococcus XMU1403 L.LI Prochlorococcus XMU1408 L.LI Prochlorococcus NATL1A L.LI Prochlorococcus NATL2A L.LI Prochlorococcus MIT0601 L.LII-III Prochlorococcus MIT0601 L.LII-III Prochlorococcus MIT0602 L.LII-III Prochlorococcus MIT0701 L.LIV Prochlorococcus MIT1312 L.LIV Prochlorococcus MIT1312		MIT9314	HLII
Prochlorococcus MIT9401 HLII Prochlorococcus SB HLII Prochlorococcus SCGCAAA795 106 HLII Prochlorococcus SCGCAAA795 115 HLII Prochlorococcus SCGCAAA795 M23 HLII Prochlorococcus HNLC1 HLIII-IV Prochlorococcus HNLC2 HLIII-IV Prochlorococcus KMU1401 HLII Prochlorococcus XMU1403 LLI Prochlorococcus MIT0801 LLI Prochlorococcus NATL1A LLI Prochlorococcus NATL1A LLI Prochlorococcus MIT0601 LLII-III Prochlorococcus MIT0602 LLII-III Prochlorococcus MIT0602 LLII-III Prochlorococcus MIT0701 LLIV Prochlorococcus MIT1312 LLIV Prochlorococcus MIT1313 LLIV Prochlorococcus MIT1318 LLIV Prochlorococcus MIT1327 LLIV Prochlorococcus </td <td></td> <td></td> <td></td>			
Prochlorococcus SB HLII Prochlorococcus SCGCAAA795 106 HLII Prochlorococcus SCGCAAA795 115 HLII Prochlorococcus SCGCAAA795 M23 HLII Prochlorococcus UH18301 HLII Prochlorococcus HNLC1 HLIII-IV Prochlorococcus HNLC2 HLIII-IV Prochlorococcus XMU1401 HLII Prochlorococcus XMU1403 LLI Prochlorococcus XMU1408 LLI Prochlorococcus NATL1A LLI Prochlorococcus NATL2A LLI Prochlorococcus MT10601 LLII-III Prochlorococcus MIT0601 LLII-III Prochlorococcus MIT0602 LLII-III Prochlorococcus MIT0701 LLIV-III Prochlorococcus MIT1312 LLIV Prochlorococcus MIT1313 LLIV Prochlorococcus MIT1318 LLIV Prochlorococcus MIT1317 LLIV Prochlorococc			
Prochlorococcus SCGCAAA795 106 HLII Prochlorococcus SCGCAAA795 115 HLII Prochlorococcus SCGCAAA795 M23 HLII Prochlorococcus UH18301 HLII Prochlorococcus HNLC1 HLIII-IV Prochlorococcus HNLC2 HLIII-IV Prochlorococcus HNLC2 HLIII-IV Prochlorococcus XMU1401 HLII Prochlorococcus XMU1403 LLI Prochlorococcus MXII 408 LLI Prochlorococcus NATL1A LLI Prochlorococcus NATL2A LLI Prochlorococcus MIT0601 LLI-III Prochlorococcus MIT0602 LLII-III Prochlorococcus MIT0911 LLII-III Prochlorococcus MIT0701 LLIV Prochlorococcus MIT1312 LLIV Prochlorococcus MIT1313 LLIV Prochlorococcus MIT1318 LLIV Prochlorococcus MIT1327 LLIV Prochloroc			
Prochlorococcus SCGCAAA795 I15 HLII Prochlorococcus SCGCAAA795 M23 HLII Prochlorococcus UH18301 HLII Prochlorococcus HNLC1 HLIII-IV Prochlorococcus HNLC2 HLIII-IV Prochlorococcus RS50 HLII Prochlorococcus XMU1401 HLII Prochlorococcus XMU1403 LLI Prochlorococcus MIT0801 LLI Prochlorococcus NATL1A LLI Prochlorococcus NATL2A LLI Prochlorococcus MIT0601 LLII-III Prochlorococcus MIT0602 LLII-III Prochlorococcus MIT0602 LLII-III Prochlorococcus MIT0701 LLIV Prochlorococcus MIT1313 LLIV Prochlorococcus MIT1313 LLIV Prochlorococcus MIT1313 LLIV Prochlorococcus MIT1318 LLIV Prochlorococcus MIT1327 LLIV Prochlorococcus			
Prochlorococcus SCGCAAA795 M23 HLII Prochlorococcus UH18301 HLII Prochlorococcus HNLC1 HLIII-IV Prochlorococcus HNLC2 HLIII-IV Prochlorococcus RS50 HLII Prochlorococcus XMU1401 HLII Prochlorococcus XMU1403 LLI Prochlorococcus MIT0801 LLI Prochlorococcus NATL1A LLI Prochlorococcus NATL2A LLI Prochlorococcus MIT0601 LLII-III Prochlorococcus MIT0602 LLII-III Prochlorococcus MIT0902 LLII-III Prochlorococcus MIT0701 LLIV Prochlorococcus MIT1312 LLIV Prochlorococcus MIT1313 LLIV Prochlorococcus MIT1318 LLIV Prochlorococcus MIT1327 LLIV Prochlorococcus MIT1323 LLIV Prochlorococcus MIT1303 LLIV Prochlorococcus			
Prochlorococcus UH18301 HLII Prochlorococcus HNLC1 HLIII-IV Prochlorococcus HNLC2 HLIII-IV Prochlorococcus HNLC2 HLIII-IV Prochlorococcus HNUC2 HLIII-IV Prochlorococcus XMU1401 HLII Prochlorococcus XMU1403 LLI Prochlorococcus MIT0801 LLI Prochlorococcus NATL1A LLI Prochlorococcus NATL2A LLI Prochlorococcus MIT0601 LLII-III Prochlorococcus MIT0602 LLII-III Prochlorococcus MIT0911 LLII-III Prochlorococcus MIT0701 LLIV-III Prochlorococcus MIT1312 LLIV Prochlorococcus MIT1313 LLIV Prochlorococcus MIT1318 LLIV Prochlorococcus MIT1327 LLIV Prochlorococcus MIT1327 LLIV Prochlorococcus MIT1303 LLIV Prochlorococcus			
Prochlorococcus HNLC1 HLIII-IV Prochlorococcus HNLC2 HLIII-IV Prochlorococcus RS50 HLII Prochlorococcus RS50 HLII Prochlorococcus XMU1401 HLII Prochlorococcus XMU1403 LLI Prochlorococcus XMU1408 LLI Prochlorococcus NATIA LLI Prochlorococcus NATLA LLI Prochlorococcus NATLA LLI Prochlorococcus MIT0601 LLII-III Prochlorococcus MIT0602 LLII-III Prochlorococcus MIT0911 LLII-III Prochlorococcus MIT0701 LLIV Prochlorococcus MIT1312 LLIV Prochlorococcus MIT1313 LLIV Prochlorococcus MIT1318 LLIV Prochlorococcus MIT1327 LLIV Prochlorococcus MIT1322 LLIV Prochlorococcus MIT1303 LLIV			
Prochlorococcus HNLC2 HLIII-IV Prochlorococcus RS50 HLII Prochlorococcus XMU1401 HLII Prochlorococcus XMU1403 LLI Prochlorococcus XMU1408 LLI Prochlorococcus MIT0801 LLI Prochlorococcus NATL1A LLI Prochlorococcus NATL2A LLI Prochlorococcus MIT0601 LLII-III Prochlorococcus MIT0602 LLII-III Prochlorococcus MIT9211 LLII-III Prochlorococcus MIT0701 LLIV Prochlorococcus MIT1313 LLIV Prochlorococcus MIT1313 LLIV Prochlorococcus MIT1318 LLIV Prochlorococcus MIT1327 LLIV Prochlorococcus MIT1342 LLIV Prochlorococcus MIT1342 LLIV Prochlorococcus MIT1303 LLIV			
Prochlorococcus RS50 HLII Prochlorococcus XMU1401 HLII Prochlorococcus XMU1403 LLI Prochlorococcus XMU1408 LLI Prochlorococcus MIT0801 LLI Prochlorococcus NATL1A LLI Prochlorococcus NATL2A LLI Prochlorococcus MIT0601 LLII-III Prochlorococcus MIT0602 LLII-III Prochlorococcus MIT9211 LLII-III Prochlorococcus MIT0701 LLIV Prochlorococcus MIT1312 LLIV Prochlorococcus MIT1313 LLIV Prochlorococcus MIT1318 LLIV Prochlorococcus MIT1327 LLIV Prochlorococcus MIT1342 LLIV Prochlorococcus MIT9303 LLIV			
Prochlorococcus XMU1401 HLII Prochlorococcus XMU1403 LLI Prochlorococcus XMU1408 LLI Prochlorococcus XMU1408 LLI Prochlorococcus XMTUA LLI Prochlorococcus NATLIA LLI Prochlorococcus NATLIA LLI Prochlorococcus MIT0601 LLII-III Prochlorococcus MIT0602 LLII-III Prochlorococcus MIT9211 LLII-III Prochlorococcus MIT0701 LLIV Prochlorococcus MIT1312 LLIV Prochlorococcus MIT1313 LLIV Prochlorococcus MIT1318 LLIV Prochlorococcus MIT1327 LLIV Prochlorococcus MIT1342 LLIV Prochlorococcus MIT9303 LLIV			
Prochlorococcus XMU1403 LLI Prochlorococcus XMU1408 LLI Prochlorococcus MIT0801 LLI Prochlorococcus NATL1A LLI Prochlorococcus NATL2A LLI Prochlorococcus MCO LLI Prochlorococcus MIT0601 LLII-III Prochlorococcus MIT0602 LLII-III Prochlorococcus MS1201 LLII-III Prochlorococcus MIT0701 LLII-III Prochlorococcus MIT1312 LLIV Prochlorococcus MIT1313 LLIV Prochlorococcus MIT1318 LLIV Prochlorococcus MIT1327 LLIV Prochlorococcus MIT1342 LLIV Prochlorococcus MIT9303 LLIV		RS50	
Prochlorococcus XMU1403 LLI Prochlorococcus XMU1408 LLI Prochlorococcus MIT0801 LLI Prochlorococcus NATL1A LLI Prochlorococcus NATL2A LLI Prochlorococcus MCO LLI Prochlorococcus MIT0601 LLII-III Prochlorococcus MIT0602 LLII-III Prochlorococcus MS1201 LLII-III Prochlorococcus MIT0701 LLII-III Prochlorococcus MIT1312 LLIV Prochlorococcus MIT1313 LLIV Prochlorococcus MIT1318 LLIV Prochlorococcus MIT1327 LLIV Prochlorococcus MIT1342 LLIV Prochlorococcus MIT9303 LLIV		XMU1401	
Prochlorococcus MIT0801 LLI Prochlorococcus NATL1A LLI Prochlorococcus NATL2A LLI Prochlorococcus NATL2A LLI Prochlorococcus MIT0601 LLII-III Prochlorococcus MIT0602 LLII-III Prochlorococcus MIT9211 LLII-III Prochlorococcus MIT0701 LLIV Prochlorococcus MIT1312 LLIV Prochlorococcus MIT1313 LLIV Prochlorococcus MIT1318 LLIV Prochlorococcus MIT1327 LLIV Prochlorococcus MIT1342 LLIV Prochlorococcus MIT9303 LLIV		XMU1403	
Prochlorococcus NATL1A LLI Prochlorococcus NATL2A LLI Prochlorococcus PAC1 LLI Prochlorococcus PAC0 LLII-III Prochlorococcus MIT0601 LLII-III Prochlorococcus MIT0602 LLII-III Prochlorococcus MIT9211 LLII-III Prochlorococcus MIT0701 LLIV Prochlorococcus MIT1312 LLIV Prochlorococcus MIT1313 LLIV Prochlorococcus MIT1318 LLIV Prochlorococcus MIT1327 LLIV Prochlorococcus MIT1342 LLIV Prochlorococcus MIT9303 LLIV			
Prochlorococcus NATL2A LLI Prochlorococcus PAC1 LLI Prochlorococcus MIT0601 LLII-III Prochlorococcus MIT0602 LLII-III Prochlorococcus MIT9211 LLII-III Prochlorococcus SS120 LLII-III Prochlorococcus MIT0701 LLIV Prochlorococcus MIT1312 LLIV Prochlorococcus MIT1313 LLIV Prochlorococcus MIT1318 LLIV Prochlorococcus MIT1327 LLIV Prochlorococcus MIT1342 LLIV Prochlorococcus MIT1303 LLIV			
Prochlorococcus PAC1 LLI Prochlorococcus MIT0601 LLII-III Prochlorococcus MIT0602 LLII-III Prochlorococcus MIT9011 LLII-III Prochlorococcus SS120 LLII-III Prochlorococcus MIT0701 LLIV Prochlorococcus MIT1312 LLIV Prochlorococcus MIT1313 LLIV Prochlorococcus MIT1318 LLIV Prochlorococcus MIT1327 LLIV Prochlorococcus MIT1342 LLIV Prochlorococcus MIT1342 LLIV Prochlorococcus MIT9303 LLIV	Prochlorococcus	NATL1A	
Prochlorococcus MIT0601 LLII-III Prochlorococcus MIT0602 LLII-III Prochlorococcus MIT0602 LLII-III Prochlorococcus MIT9211 LLII-III Prochlorococcus MIT0701 LLIV Prochlorococcus MIT1312 LLIV Prochlorococcus MIT1313 LLIV Prochlorococcus MIT1318 LLIV Prochlorococcus MIT1327 LLIV Prochlorococcus MIT1342 LLIV Prochlorococcus MIT9303 LLIV	Prochlorococcus		
Prochlorococcus MIT0601 LLII-III Prochlorococcus MIT0602 LLII-III Prochlorococcus MIT0602 LLII-III Prochlorococcus MIT9211 LLII-III Prochlorococcus MIT0701 LLIV Prochlorococcus MIT1312 LLIV Prochlorococcus MIT1313 LLIV Prochlorococcus MIT1318 LLIV Prochlorococcus MIT1327 LLIV Prochlorococcus MIT1342 LLIV Prochlorococcus MIT9303 LLIV	Prochlorococcus	PAC1	LLI
Prochlorococcus MIT0602 LLII-III Prochlorococcus MIT9211 LLII-III Prochlorococcus SS120 LLII-III Prochlorococcus MIT0701 LLIV Prochlorococcus MIT1312 LLIV Prochlorococcus MIT1313 LLIV Prochlorococcus MIT1318 LLIV Prochlorococcus MIT1327 LLIV Prochlorococcus MIT1342 LLIV Prochlorococcus MIT9303 LLIV			
Prochlorococcus MIT9211 LLII-III Prochlorococcus SS120 LLII-III Prochlorococcus MIT0701 LLIV Prochlorococcus MIT1312 LLIV Prochlorococcus MIT1313 LLIV Prochlorococcus MIT1318 LLIV Prochlorococcus MIT1327 LLIV Prochlorococcus MIT1342 LLIV Prochlorococcus MIT9303 LLIV			
Prochlorococcus SS120 LLII-III Prochlorococcus MIT0701 LLIV Prochlorococcus MIT1312 LLIV Prochlorococcus MIT1313 LLIV Prochlorococcus MIT1318 LLIV Prochlorococcus MIT1327 LLIV Prochlorococcus MIT1342 LLIV Prochlorococcus MIT9303 LLIV			
Prochlorococcus MIT0701 LLIV Prochlorococcus MIT1312 LLIV Prochlorococcus MIT1313 LLIV Prochlorococcus MIT1318 LLIV Prochlorococcus MIT1327 LLIV Prochlorococcus MIT1342 LLIV Prochlorococcus MIT9303 LLIV			
Prochlorococcus MIT1312 LLIV Prochlorococcus MIT1313 LLIV Prochlorococcus MIT1318 LLIV Prochlorococcus MIT1327 LLIV Prochlorococcus MIT1342 LLIV Prochlorococcus MIT9303 LLIV			
Prochlorococcus MIT1313 LLIV Prochlorococcus MIT1318 LLIV Prochlorococcus MIT1327 LLIV Prochlorococcus MIT1342 LLIV Prochlorococcus MIT9303 LLIV			
Prochlorococcus MIT1318 LLIV Prochlorococcus MIT1327 LLIV Prochlorococcus MIT1342 LLIV Prochlorococcus MIT9303 LLIV			
Prochlorococcus MIT1327 LLIV Prochlorococcus MIT1342 LLIV Prochlorococcus MIT9303 LLIV			
Prochlorococcus MIT1342 LLIV Prochlorococcus MIT9303 LLIV			
Prochlorococcus MIT9303 LLIV			
	Prochlorococcus		
Prochlorococcus MIT9313 LLIV			
	Prochlorococcus	MIT9313	LLIV

Supplementary Table 5: Descriptions, values, and units of fixed model parameters.

Parameter	Description	Units	Value
$D_{ m N}$	Diffusivity of Nitrate at 25°	$10^{-3} {\rm m}^2/{\rm hr}$	1.6×10^{-9}
$D_{ m P}$	Diffusivity of Phosphate at 25°	$10^{-3}\mathrm{m}^2/\mathrm{hr}$	1.6×10^{-9}
$Q_{10,D}$	Q_{10} for diffusivity		1.5
$Q_{10,k}$	Q_{10} for biosynthesis		2.0
$p_{ m dry}$	Dry mass fraction of the cell		0.47
P_{DNA}	Phosphorus mass fraction in DNA	gP/g	0.095
$P_{\rm rib}$	Phosphorus mass fraction in ribosomes	gP/g	0.047
N_{prot}	Nitrogen mass fraction in proteins	gN/g	0.16
N_{DNA}	Nitrogen mass fraction in DNA	gN/g	0.16
$N_{\rm rib}$	Nitrogen mass fraction in ribosomes	gN/g	0.16
C_{prot}	Carbon mass fraction in proteins	gC/g	0.53
C_{lipid}	Carbon mass fraction in lipids	gC/g	0.76
C_{DNA}	Carbon mass fraction in DNA	gC/g	0.36
$\mathrm{mol}_{\mathrm{P}}$	Molar mass of Phosphorus	g/mol	31.0
$\mathrm{mol}_{\mathrm{N}}$	Molar mass of Nitrogen	g/mol	14.0
$\mathrm{mol}_{\mathrm{C}}$	Molar mass of Carbon	g/mol	12.0
$f_{ m prot}$	Protein fraction of cell membranes		0.25
$f_{ m prot L}$	Protein fraction of light harvesting apparatus		0.70
Φ_S	Specific Carbon cost of synthesis	gC/gC	0.67
$D_{ m N}$	Diffusivity of Nitrate at 25°	$10^{-3}\mathrm{m}^2/\mathrm{hr}$	1.6×10^{-9}
$D_{ m P}$	Diffusivity of Phosphate at 25°	$10^{-3}\mathrm{m}^2/\mathrm{hr}$	1.6×10^{-9}
$Q_{10,D}$	Q_{10} for diffusivity		1.5
$Q_{10,k}$	Q_{10} for biosynthesis		2.0
$p_{ m dry}$	Dry mass fraction of the cell		0.47
P_{DNA}	Phosphorus mass fraction in DNA	gP/g	0.095
$P_{\rm rib}$	Phosphorus mass fraction in ribosomes	gP/g	0.047
N_{prot}	Nitrogen mass fraction in proteins	gN/g	0.16
N_{DNA}	Nitrogen mass fraction in DNA	gN/g	0.16
$N_{\rm rib}$	Nitrogen mass fraction in ribosomes	gN/g	0.16
C_{prot}	Carbon mass fraction in proteins	gC/g	0.53
C_{lipid}	Carbon mass fraction in lipids	gC/g	0.76
C_{DNA}	Carbon mass fraction in DNA	gC/g	0.36
$\mathrm{mol}_{\mathrm{P}}$	Molar mass of Phosphorus	g/mol	31.0
$\mathrm{mol}_{\mathrm{N}}$	Molar mass of Nitrogen	g/mol	14.0
$\mathrm{mol}_{\mathrm{C}}$	Molar mass of Carbon	g/mol	12.0
$f_{ m prot}$	Protein fraction of cell membranes		0.7
Φ_S	Specific Carbon cost of synthesis	gC/gC	0.67

Supplementary Table 6: Prior probability distribution and model parameter description for ATOM-gene

Parameter	Description	Units	Prior
$Q_{10,\mathrm{photo}}$	Q_{10} of photosynthesis		Unif $(1.0, 2.0)$
α_E	Ribosome fraction of synthetic apparatus		$\mathrm{Unif}(0.3, 1.0)$
α_S	Radius at which cell is all periplasm and membrane	$\mu\mathrm{m}$	Unif(0.15, 0.50)
k_{ST0}	Specific Synthesis rate of synthetic apparatus at 25°	$1/\mathrm{hr}$	Unif(0.01, 0.35)
$\gamma_{ m DNA}$	DNA fraction of cell		Unif(0.0, 0.05)
A_{\min}	Minimal allocation to periplasmic uptake proteins		$\mathrm{Unif}(0.0, 1.0)$
γ	Mass fraction of other structural components		$\mathrm{Unif}(0.1,0.3)$
μ_c	Growth cutoff above which luxury storage does not occur	1/day	$\mathrm{Unif}(0.0, 1.0)$
$f_{ m stor}$	Strength of luxury P storage	L/molC	$\mathrm{Unif}(0.0, 5 \times 10^4)$
N_{0L}	Intercept in gene-N prediction model	$\log_{10}(\mathrm{molN/L})$	Unif(-7, -5)
P_{0L}	Intercept in gene-P prediction model	$\log_{10}(\mathrm{molP/L})$	Unif(-8, -6)
$C_{ m N}$	Relationship between N-genes and N availability	$\log_{10}(\mathrm{molN/L})$	$\mathrm{Unif}(1,4)$
C_{P}	Relationship between P-genes and P availability	$\log_{10}(\mathrm{molP/L})$	Unif(1,4)

Supplementary Table 7: Model comparison using information criteria derived from leave-one-out cross validation (loo-cv), calculated using Pareto Smoothed Importance Sampling (Vehtari et. al. 2017). Lower numbers suggest better out of sample performance. P_waic estimates effective number of model parameters.

Model	Rank	waic	p_waic	weight	se
Syn. Genes	1	-36.3739	7.04761	0.95492	14.225
Pro. Genes	2	-21.788	5.098	0.0255918	12.0595
T. Reg	3	-17.067	3.7877	0.0151752	13.9073
P. Reg	4	-12.0807	3.6576	0.0028125	14.5828
Trait Nutrient	5	-11.0926	3.64052	0.0015	13.8015

Supplementary Table 8: Fit summary for ATOM-gene model based on Synechococcus gene indices.

Parameter	Mean	$\mathrm{se}_{\mathrm{mean}}$	sd	2.5%	25%	50%	75%	97.5%	n_{eff}	\hat{R}
$Q_{10Photo}$	1.71	0.0008	0.21	1.20	1.59	1.74	1.87	1.99	68115	1.00
α_E	0.58	0.0009	0.20	0.31	0.40	0.55	0.73	0.96	48519	1.00
f_{Stor}	3.87	0.012	3.01	0.12	1.08	3.23	6.37	9.62	61137	1.00
σ_{PC}	0.17	0.00009	0.022	0.14	0.16	0.17	0.19	0.22	67848	1.00
α_S	0.17	0.0003	0.074	0.10	0.12	0.15	0.20	0.38	83546	1.00
$\gamma_{ m DNA}$	0.033	0.00005	0.013	0.0038	0.025	0.037	0.044	0.049	83496	1.00
γ	0.20	0.0002	0.057	0.11	0.16	0.21	0.25	0.30	109790	1.00
A_{\min}	0.48	0.0009	0.30	0.019	0.21	0.47	0.74	0.97	101914	1.00
μ_C	0.33	0.0012	0.25	0.013	0.13	0.27	0.47	0.90	39307	1.00
N_{0L}	-5.82	0.0018	0.50	-6.82	-6.19	-5.79	-5.41	-5.04	77370	1.00
P_{0L}	-6.44	0.0012	0.33	-7.21	-6.65	-6.38	-6.17	-6.02	79733	1.00
C_{ProN}	1.53	0.0014	0.38	1.02	1.22	1.47	1.78	2.37	75134	1.00
C_{ProP}	1.21	0.00057	0.17	1.01	1.07	1.16	1.30	1.61	83768	1.00

Supplementary Table 9: Fit summary for ATOM-gene model based on Prochlorococcus gene indices.

Parameter	Mean	se_{mean}	sd	2.5%	25%	50%	75%	97.5%	n_{eff}	\hat{R}
$Q_{10\mathrm{photo}}$	1.68	0.00	0.22	1.16	1.54	1.71	1.86	1.99	40283	1.00
α_E	0.59	0.00	0.19	0.31	0.42	0.57	0.75	0.96	52962	1.00
$f_{ m stor}$	3.75	0.01	2.95	0.07	1.07	3.11	6.12	9.57	58790	1.00
$\sigma_{ m CP}$	0.14	0.00	0.02	0.11	0.13	0.14	0.15	0.18	63347	1.00
$lpha_S$	0.24	0.00	0.11	0.10	0.15	0.22	0.31	0.47	88589	1.00
$\gamma_{ m DNA}$	0.03	0.00	0.01	0.00	0.02	0.04	0.04	0.05	93835	1.00
γ	0.20	0.00	0.06	0.11	0.15	0.20	0.25	0.30	117586	1.00
A_{\min}	0.47	0.00	0.30	0.02	0.20	0.46	0.73	0.97	107015	1.00
μ_C	0.43	0.00	0.27	0.02	0.19	0.39	0.65	0.95	26373	1.00
N_{0L}	-6.07	0.00	0.54	-6.94	-6.52	-6.10	-5.63	-5.08	75875	1.00
P_{0L}	-6.90	0.00	0.52	-7.84	-7.31	-6.91	-6.47	-6.05	35628	1.00
$C_{ m synN}$	2.27	0.00	0.71	1.11	1.71	2.22	2.79	3.72	65479	1.00
C_{synP}	1.73	0.00	0.57	1.03	1.28	1.60	2.07	3.09	34158	1.00